

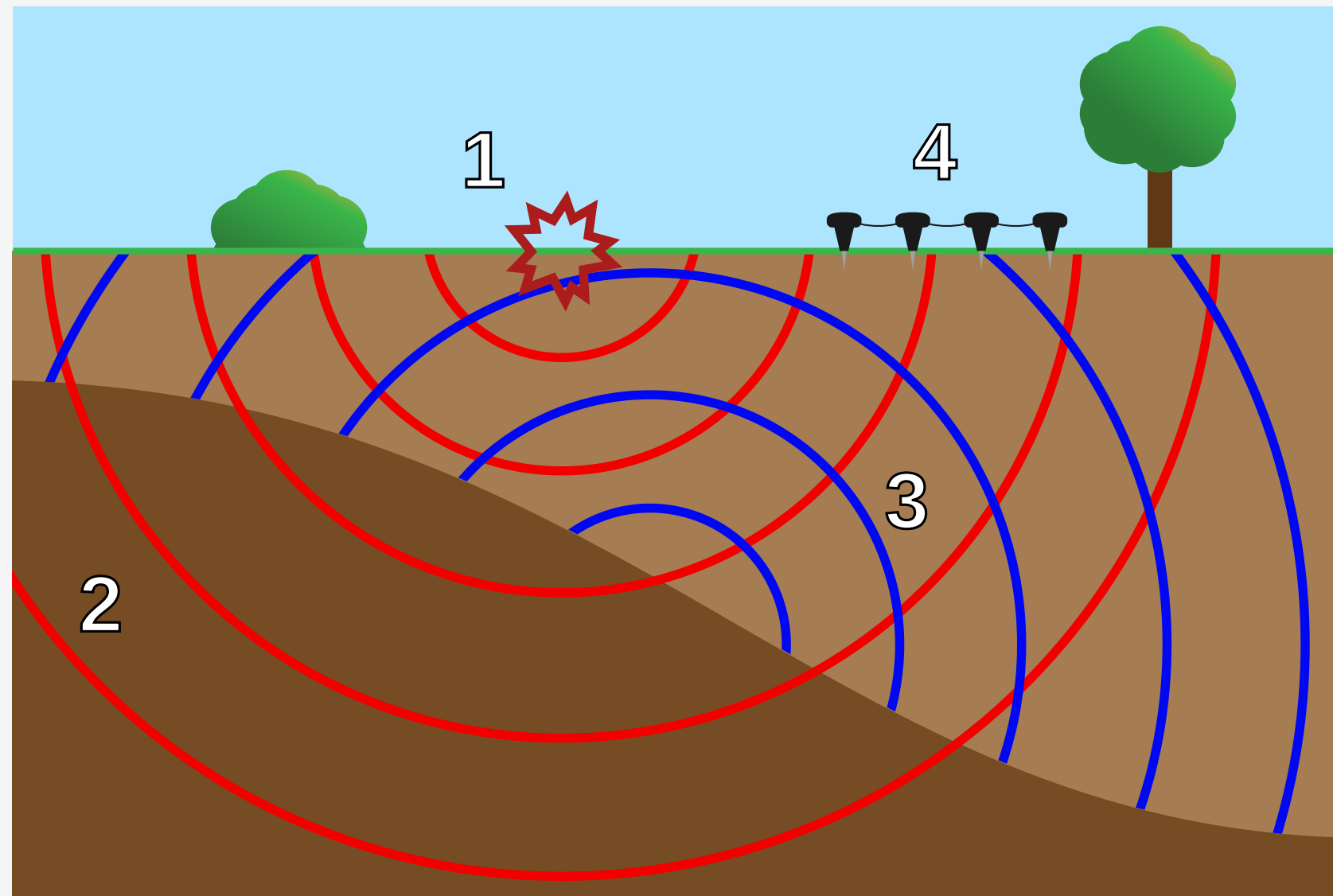
COMPUTATIONALLY EFFICIENT METHODS FOR UNCERTAINTY QUANTIFICATION IN SEISMIC INVERSION



Georgia K. Stuart

The Department of Mathematical Sciences
The University of Texas at Dallas

28 September 2020



1. A **seismic disturbance**.
2. **Seismic waves** propagating through the subsurface.
3. **Reflected seismic waves** created by the change in material.
4. **Geophones** that record the direct (red) and reflected (blue) waves.

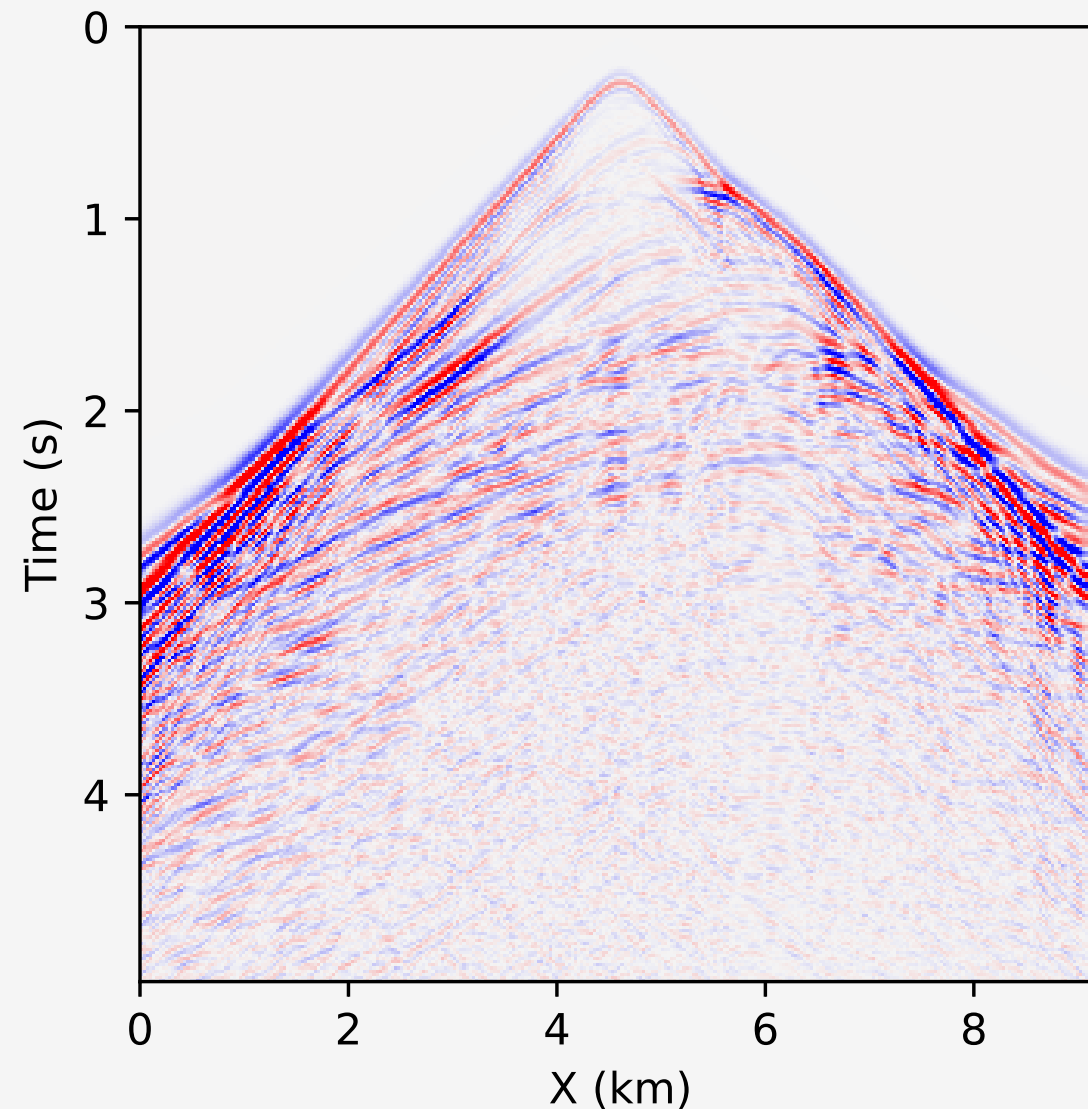


Figure: Synthetic receiver data with a t^2 gain applied to emphasize the later events.

✚ In **Full Waveform Inversion (FWI)**, the goal is to **minimize** an objective function, e.g.:

$$\frac{1}{2} \|F(\theta) - D\|^2$$

where θ describes the velocity field, D is the observed seismic data, and $F(\theta)$ is the simulated seismic data.

✚ We use the **2D constant-density acoustic wave equation**:

$$\frac{1}{c^2(x, z)} \frac{\partial^2 p}{\partial t^2} - \Delta p = f$$

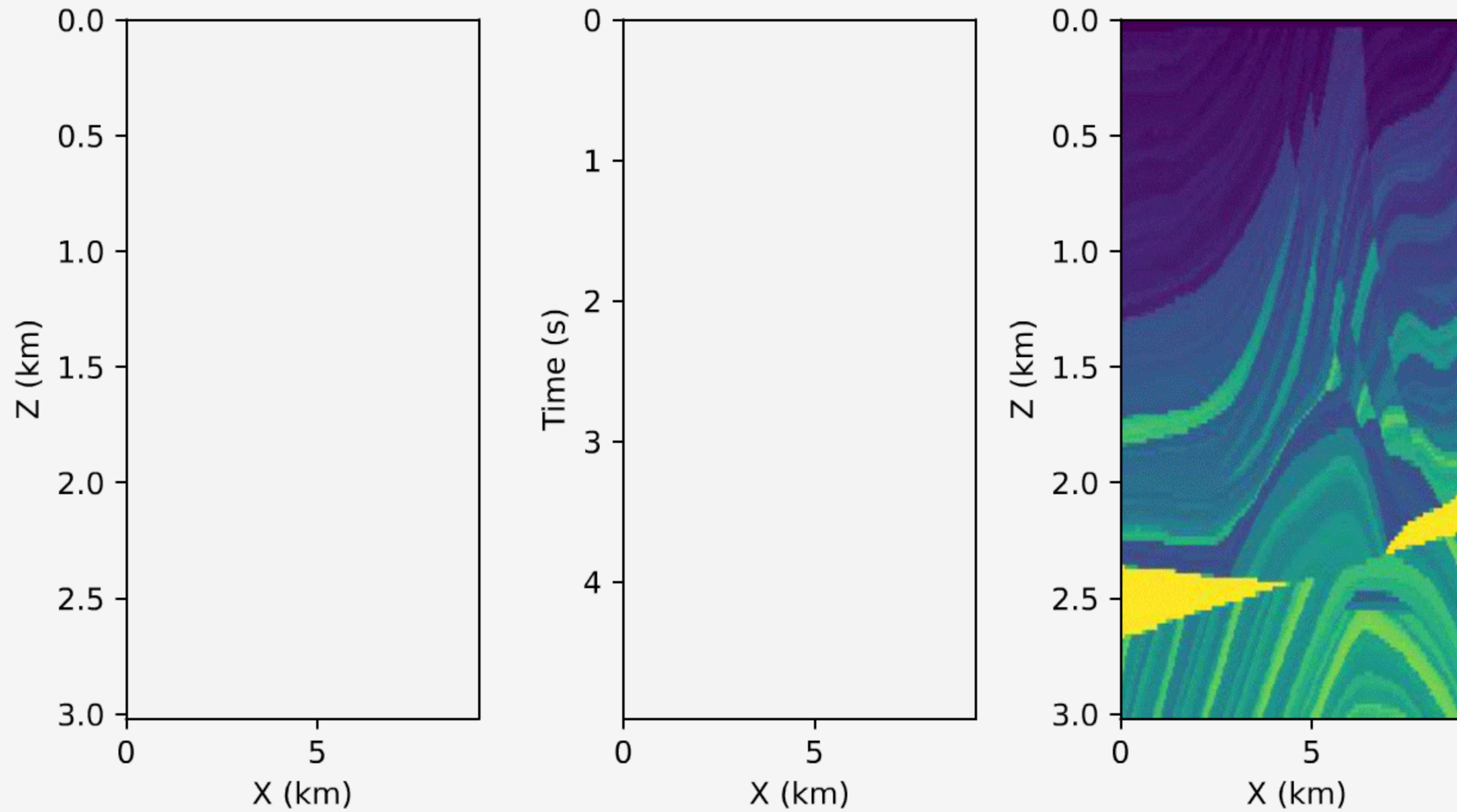
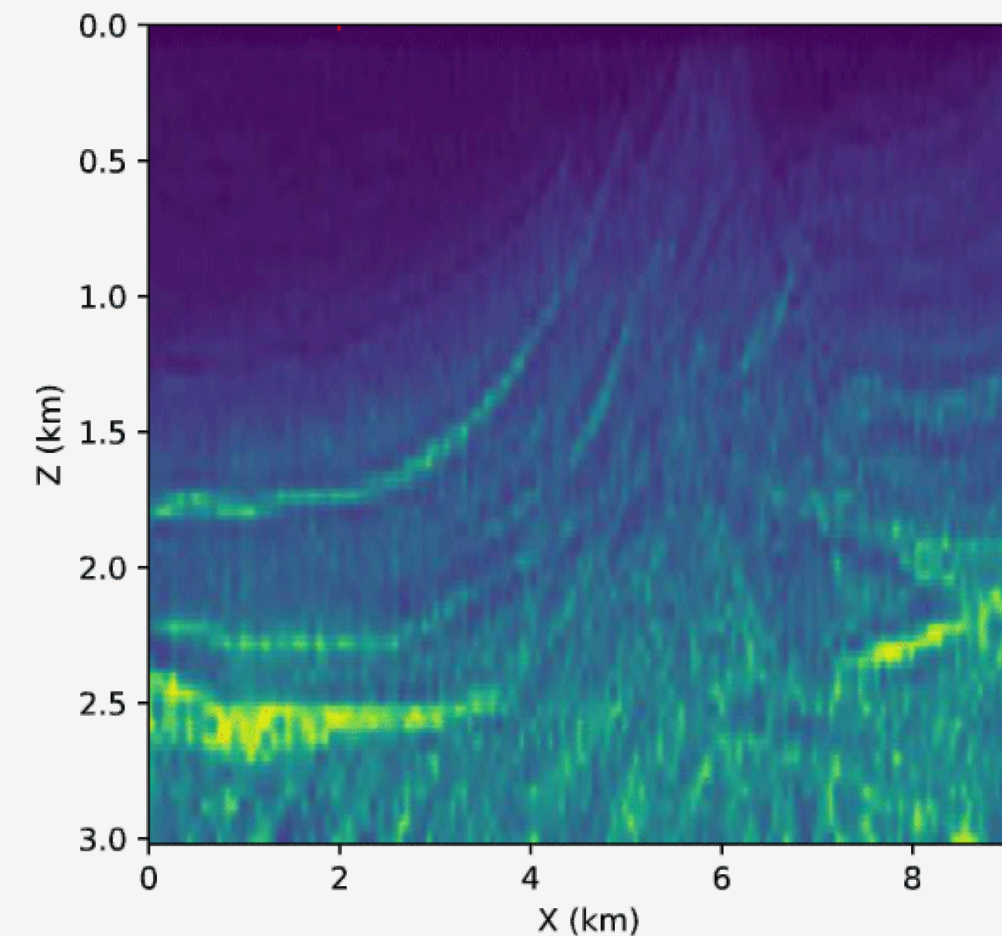


Figure: Left: an acoustic wave propagating through the velocity field on the right. Center: Receiver data by time. Right: the velocity profile.

- Traditional FWI methods result in a **single velocity field**.
- UQ methods result in **distributions of velocity fields**.
- UQ indicates where we have **more or less certainty** about the estimate from FWI.



BAYES' RULE



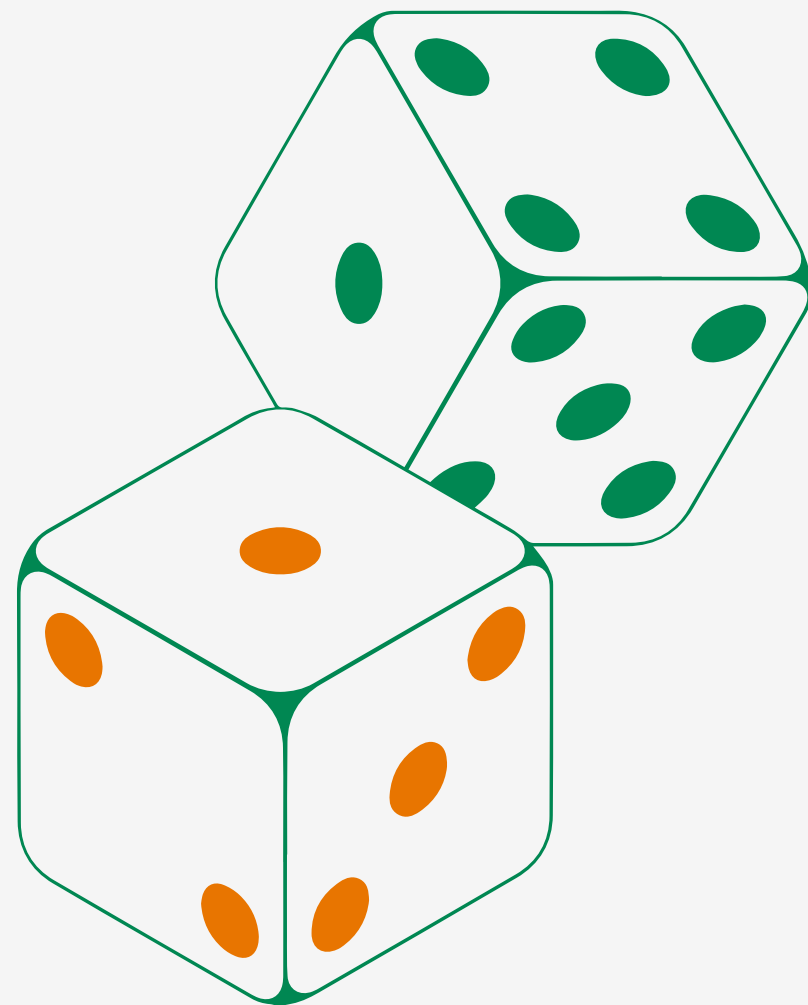
↯ We assume the **likelihood function** has the form

$$\pi(D|\theta) = \exp \left(-\frac{\|F(\theta) - D\|^2}{2\sigma^2} \right)$$

where $F(\theta)$ is the simulated data, D is the observed data, and σ is the precision parameter.

↯ The **prior distribution** can take many forms, e.g. uniform or Gaussian.

↯ However, the **posterior is not necessarily Gaussian**.



- ↯ **Deterministic** approaches to Bayesian FWI require **many assumptions**.
- ↯ **Stochastic** approaches require fewer assumptions.
- ↯ **Markov chain Monte Carlo** methods sample from the posterior distribution **without assumptions** on the shape of the distribution.

MARKOV CHAIN MONTE CARLO (MCMC)



START

STOP

RESET

- ⚡ MCMC can take **many models (tens of thousands to millions)** to converge.
- ⚡ Each model must be run through a forward simulator (**wave equation**).
- ⚡ A single chain can take **a week or more** on a cluster.
- ⚡ Often **80% to 90%** of the samples are rejected!

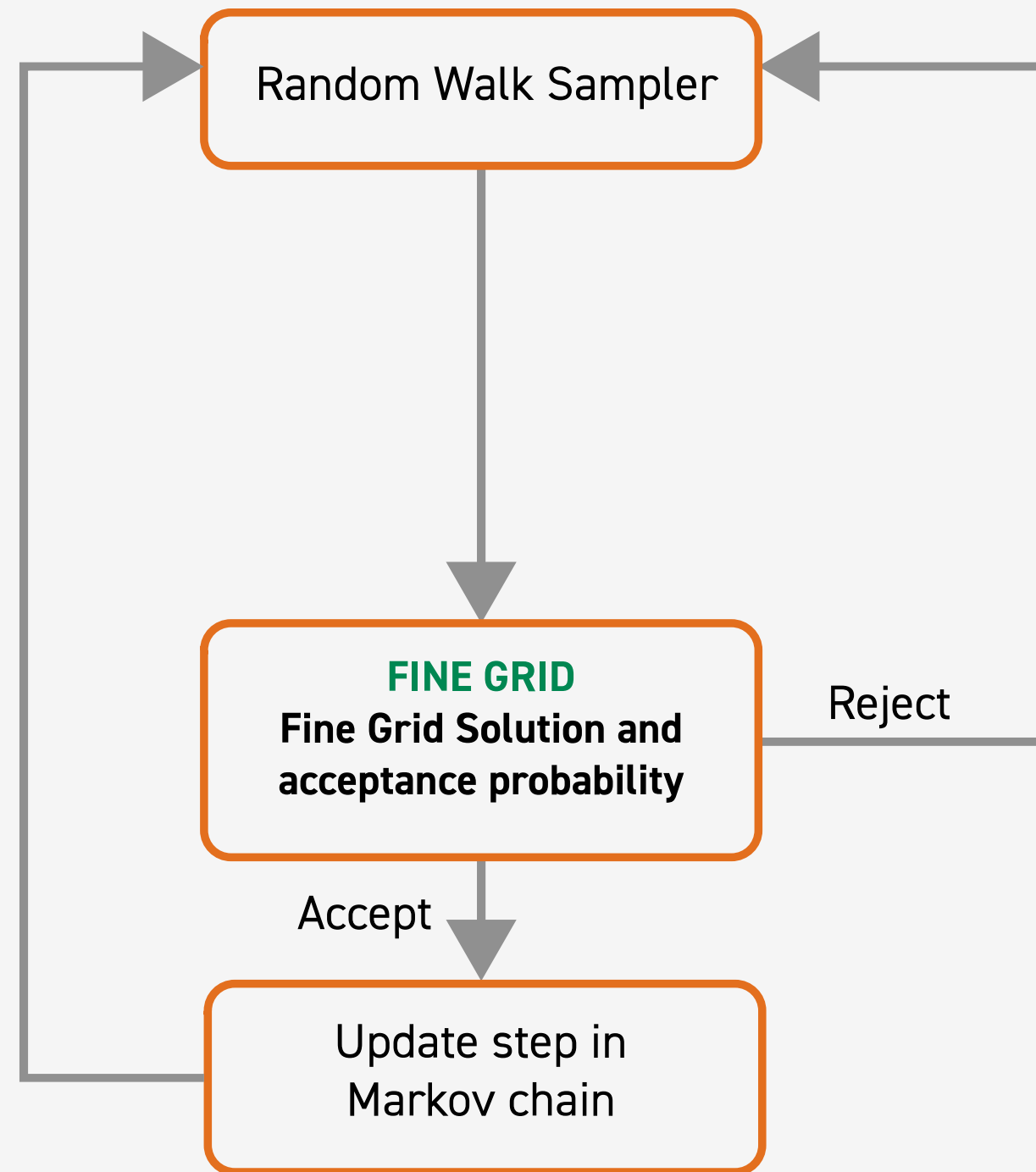


HOW CAN WE REDUCE THE
COMPUTATIONAL COST OF
MCMC METHODS FOR FWI?

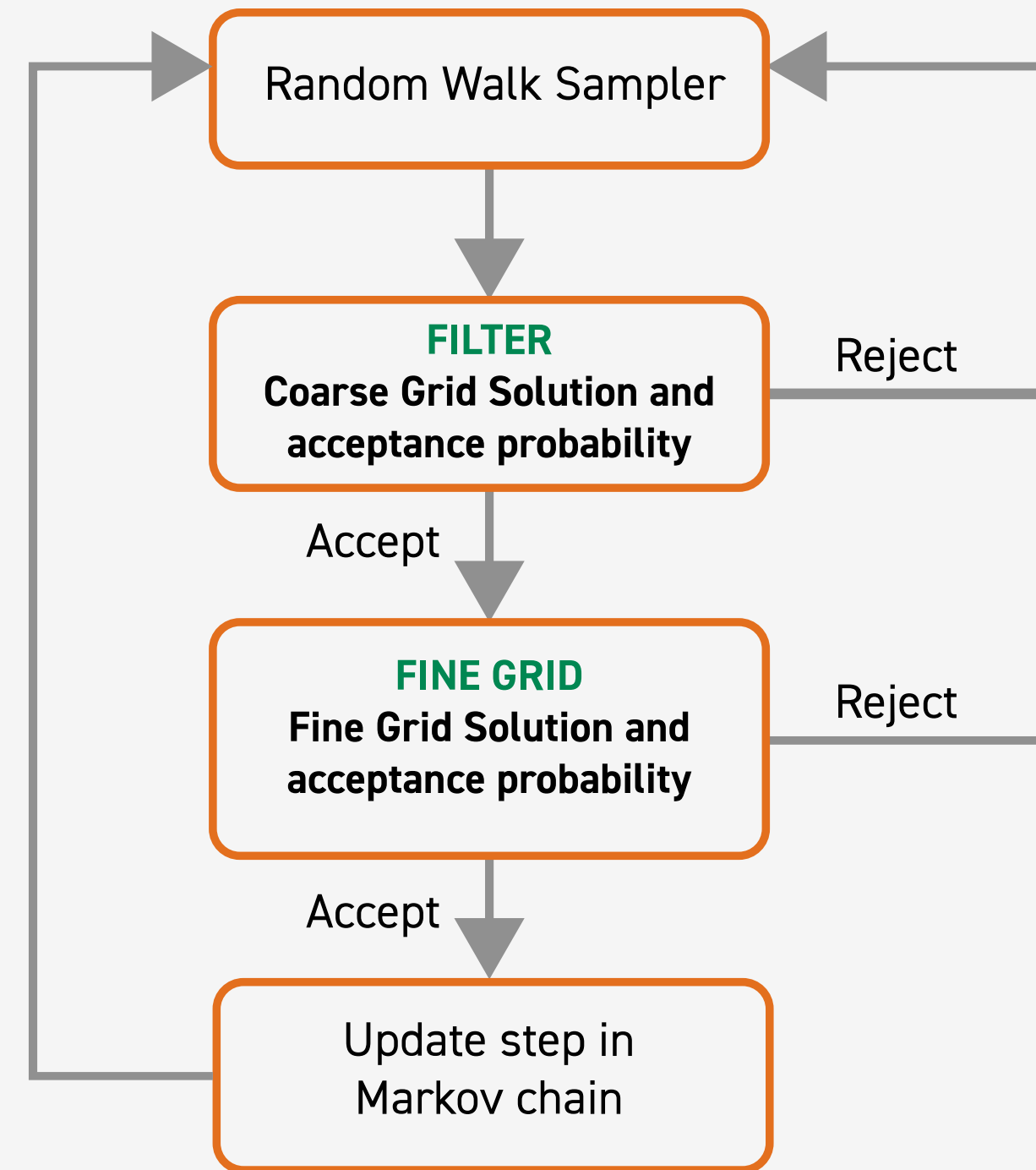
TWO-STAGE MARKOV CHAIN MONTE CARLO



ONE STAGE MCMC



TWO-STAGE MCMC



⚡ Modeling wave propagation can be **computationally expensive**.

⚡ **Operator upscaling**¹ decomposes the solution into two parts:

1. **Fine grid** problem on independent subdomains
2. Small **coarse grid** problem over the whole domain

⚡ In this upscaling technique **we do NOT upscale the model**.

(1) Vdovina et al. (2005), Korostyshevskaya and Minkoff (2006), Vdovina and Minkoff (2008)

1. Write the acoustic wave equation as a system in space by introducing **acceleration, \vec{v}**

$$\vec{v} = -\nabla p$$

$$\frac{1}{c^2} \frac{\partial^2 p}{\partial t^2} = -\nabla \cdot \vec{v} + f$$

2. Solve in parallel for fine grid pressure and acceleration over each **independent** coarse block. **No communication** is required at this stage.

3. Solve for coarse grid acceleration over the whole domain.

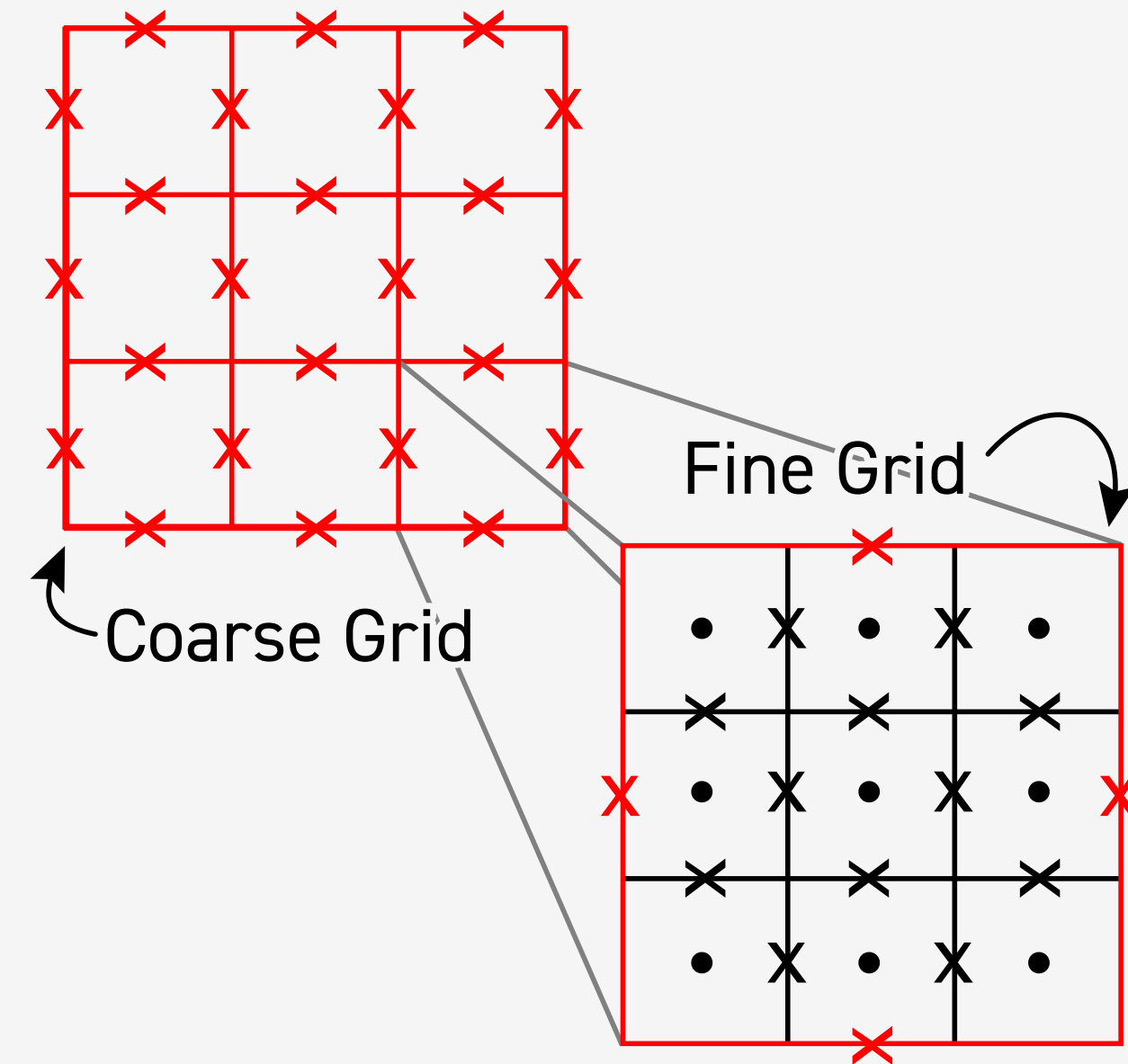
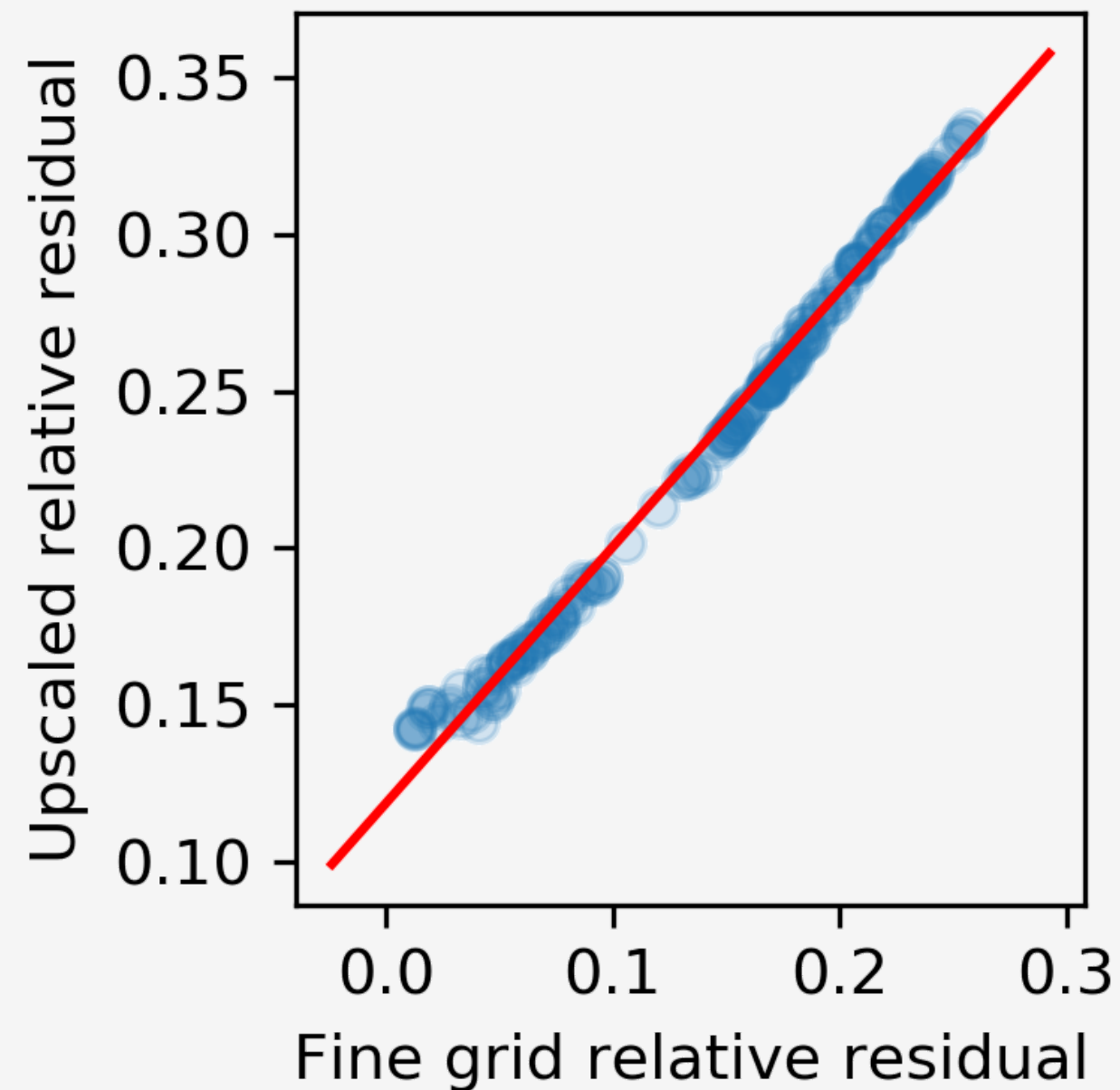


Figure: A picture of the coarse grid (red) and coarse grid acceleration (red X's) and the fine grid (black) and fine grid unknowns (black X's: acceleration, black dots: pressure)



- ✓ We see a **strong linear relationship** between the fine grid relative residuals and the upscaled relative residuals for a layered velocity model.
- ✓ This indicates that the upscaling filter is a **good surrogate** for the fine grid solver.

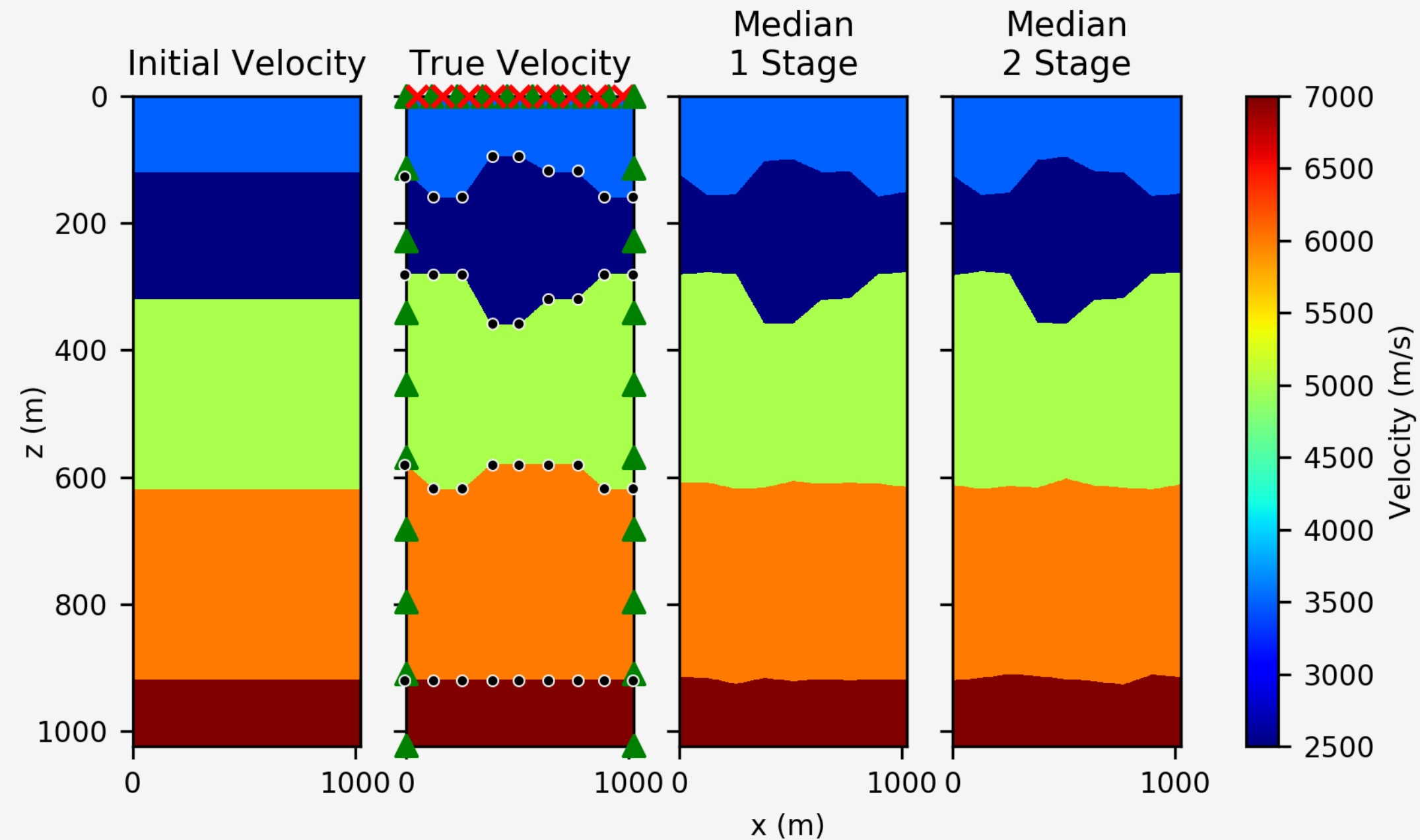


Figure: A comparison of the initial velocity, true velocity, median of the posterior from one-stage MCMC, and the median of the posterior distribution from two-stage MCMC. The true velocity shows the location of a line of sources (red X's), receivers (green triangles), and the unknown nodes that describe the interfaces (black dots). Published in Stuart (2019b).

RESULTS: TWO-STAGE MCMC WITH UPSCALING

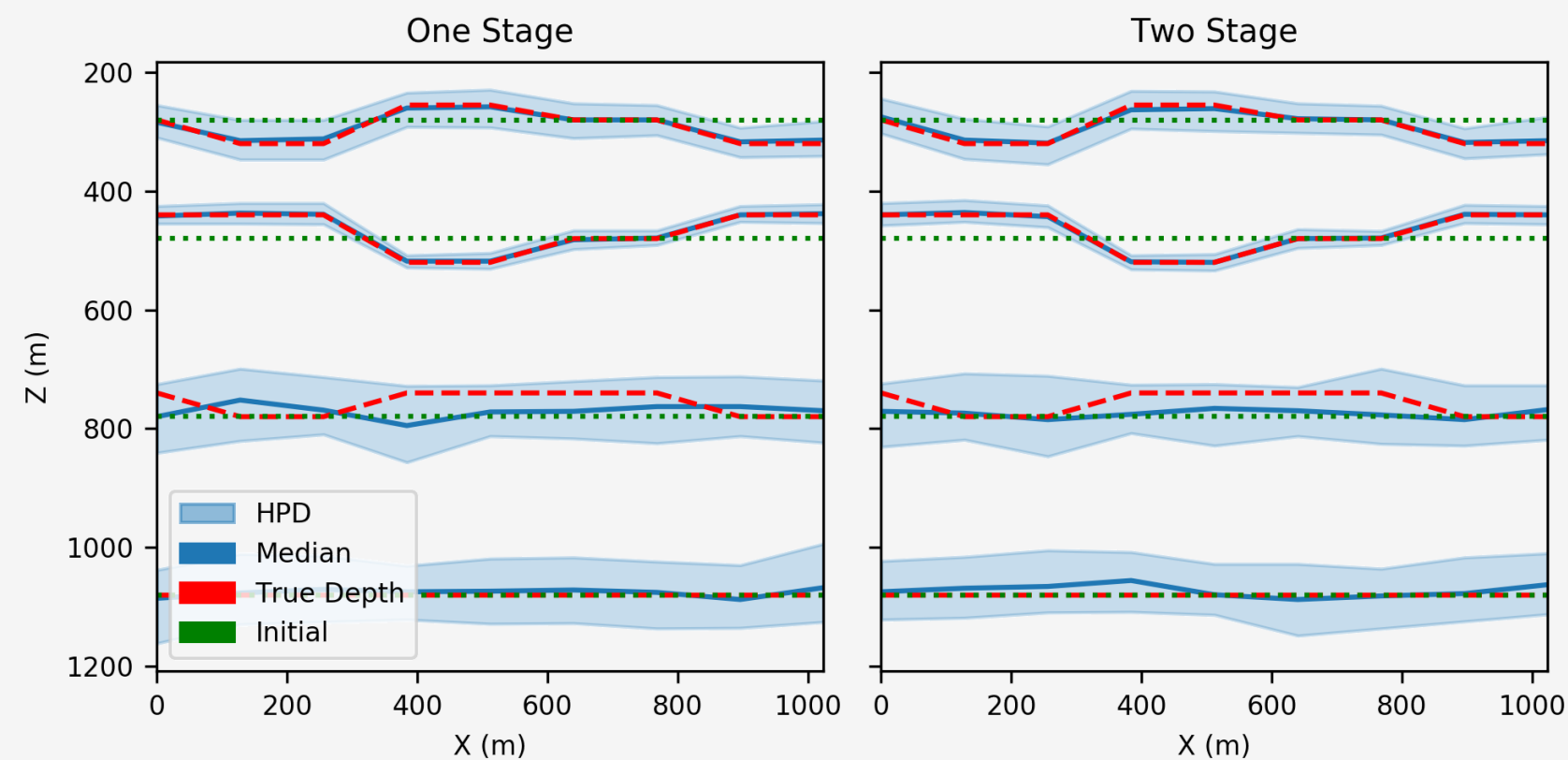


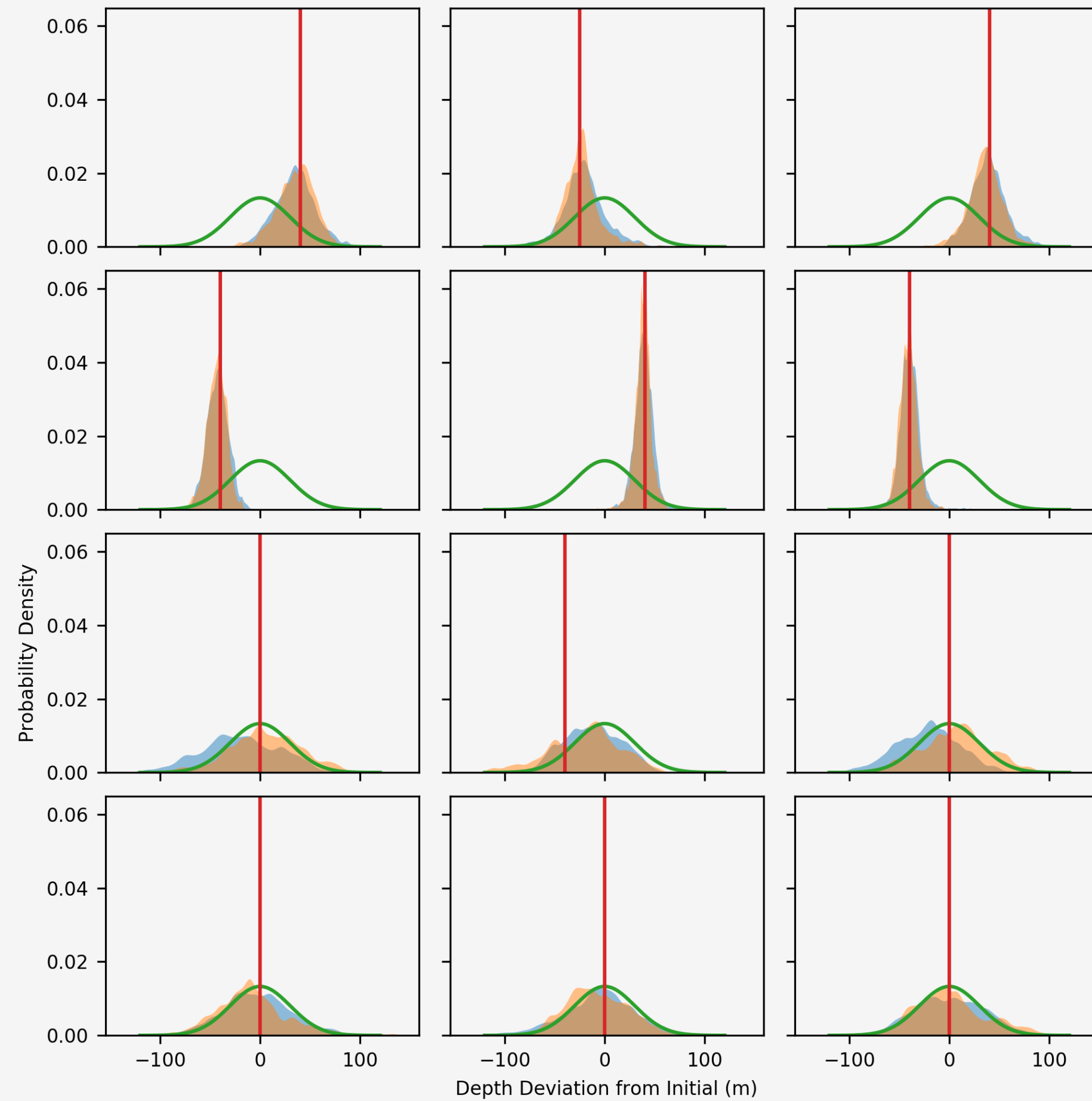
Figure: A comparison between one-stage MCMC highest posterior density (HPD) intervals and two-stage MCMC HPD intervals.

✓ Acceptance rate
increased from 10% to 40%.

✓ Time per sample
decreased by 22%
(40% in other experiments).

✓ Time per rejection
decreased by 33%.

RESULTS: TWO-STAGE MCMC WITH UPSCALING

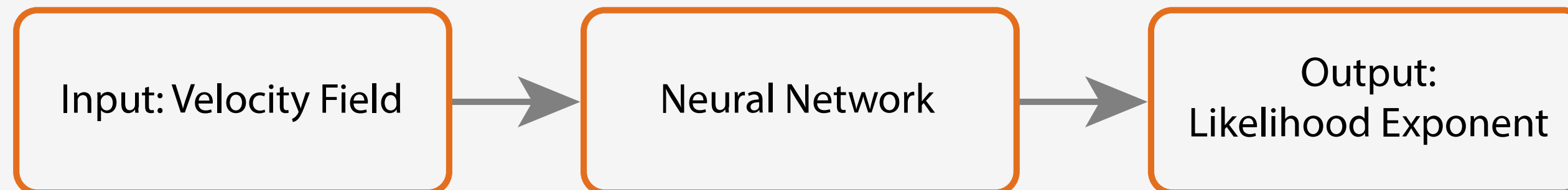


✚ The **likelihood function** is:

$$\exp \left(-\frac{\|F(\theta) - D\|^2}{2\sigma^2} \right)$$

where θ is the velocity field, $F(\theta)$ is the simulated data, and D is the observed data.

✚ Idea: replace the **likelihood exponent** with a neural network.



PROS

- ⚡ Evaluating a model is **extremely fast** (< 1 second).
- ⚡ Neural networks are capable of approximating **very complex relationships**.
- ⚡ Data for training can be generated **as part of the MCMC process**.

CONS

- ⚡ Where's the **physics**?
- ⚡ Training data is **expensive** to generate
- ⚡ Predictions are not always very accurate **very complex relationships**.
- ⚡ Many **knobs to twist** in the neural network!

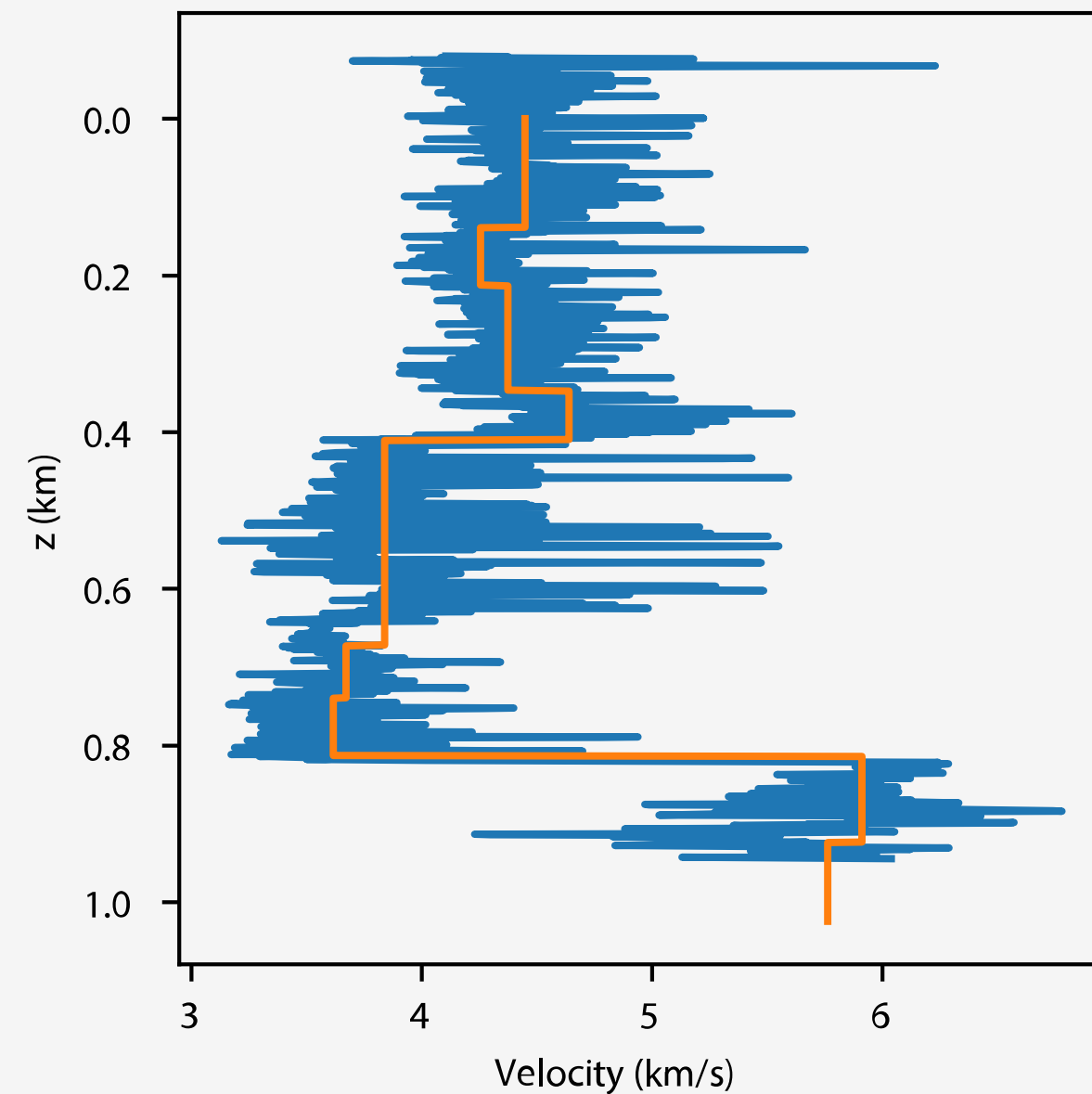


Figure: Well log from the Midland, TX basin (blue, courtesy of Pioneer Natural Resources and 9-layer block (orange).

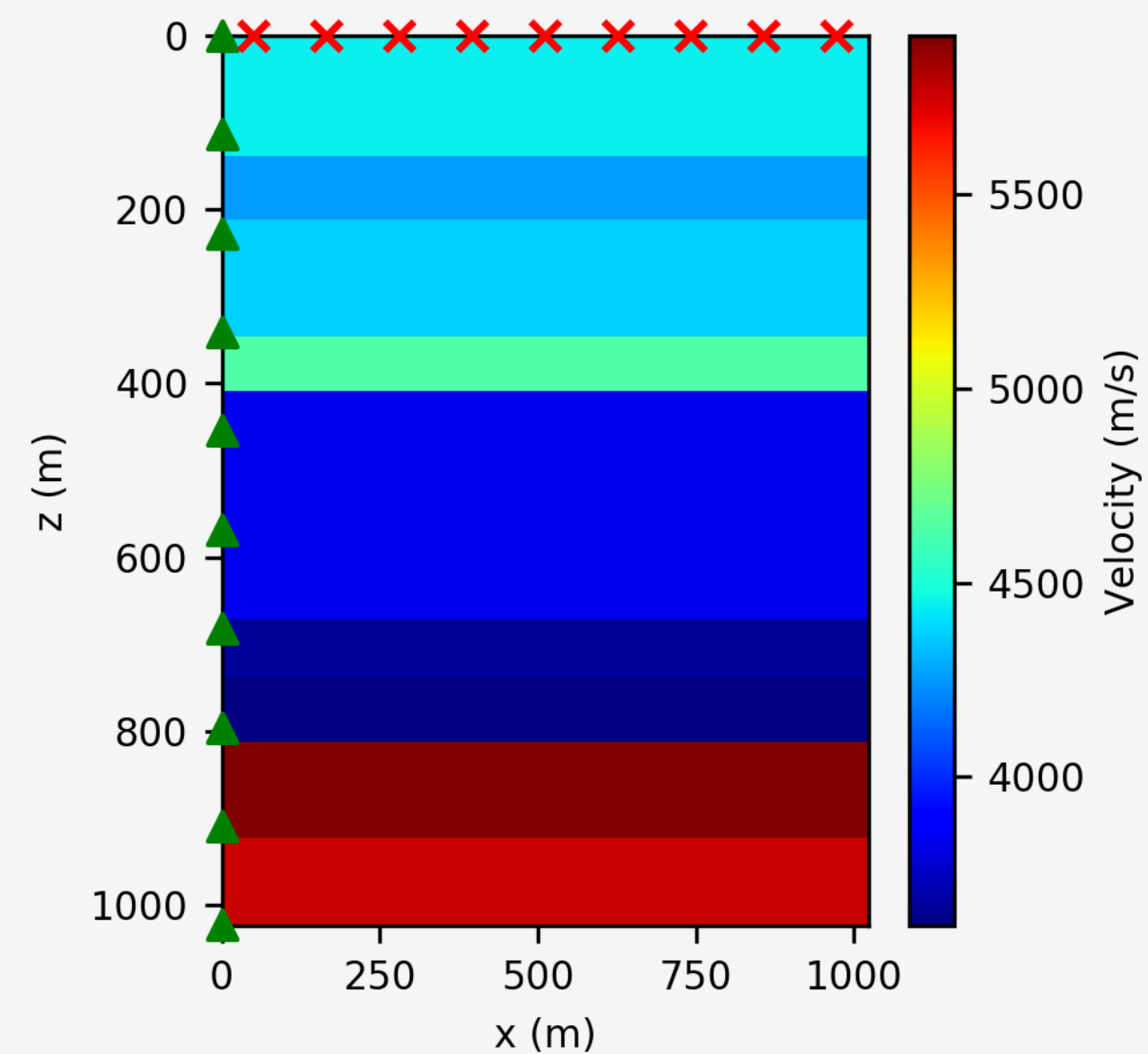


Figure: Flat layered experimental setup with nine unknowns (Stuart et al. 2019a)

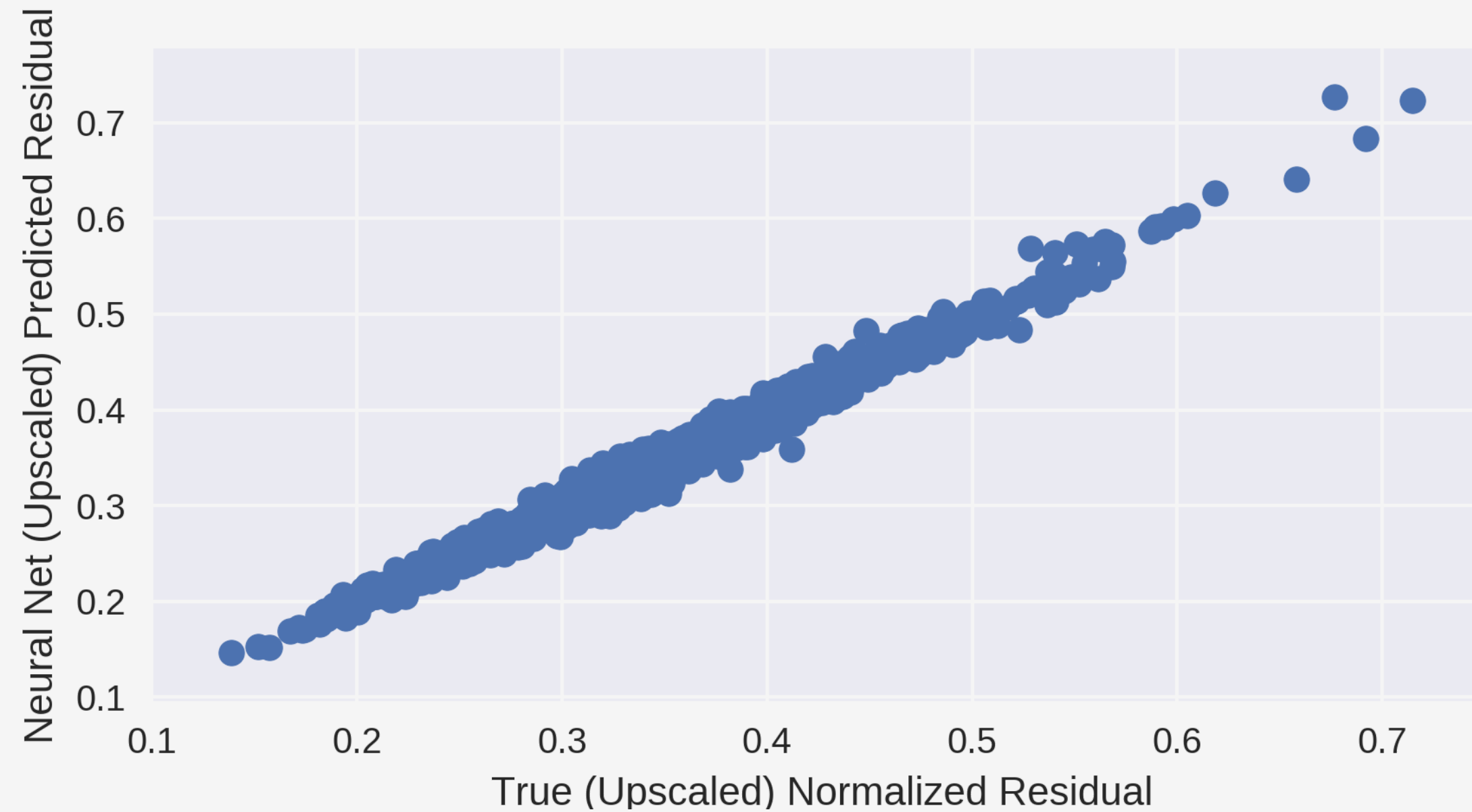


Figure: The fine grid residual norm vs. neural network filter residual norm with continuous learning.

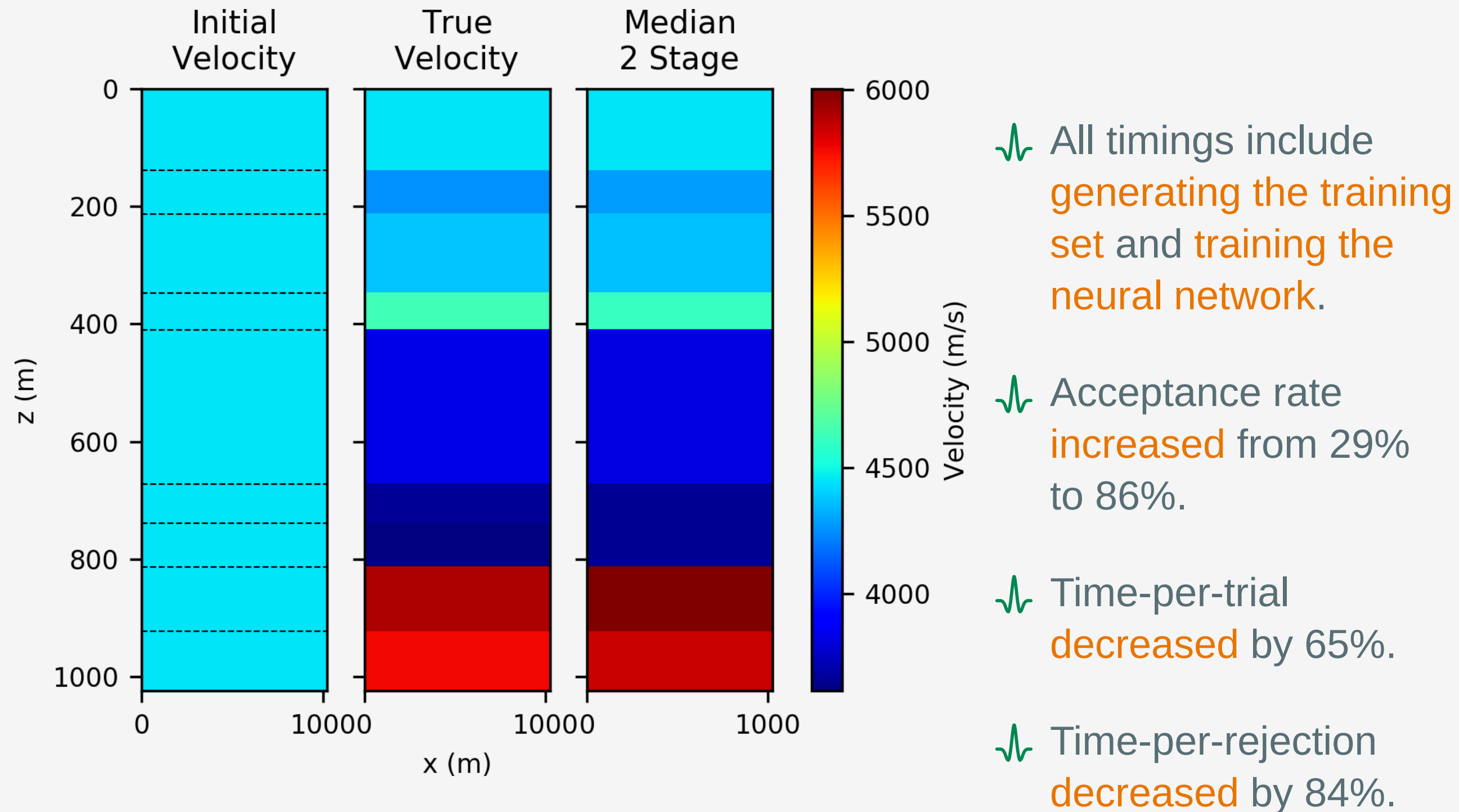


Figure: The initial, true, and median velocity fields for the neural net two-stage MCMC experiment. The dashed lines in the initial velocity field mark the positions of pre-set interfaces.

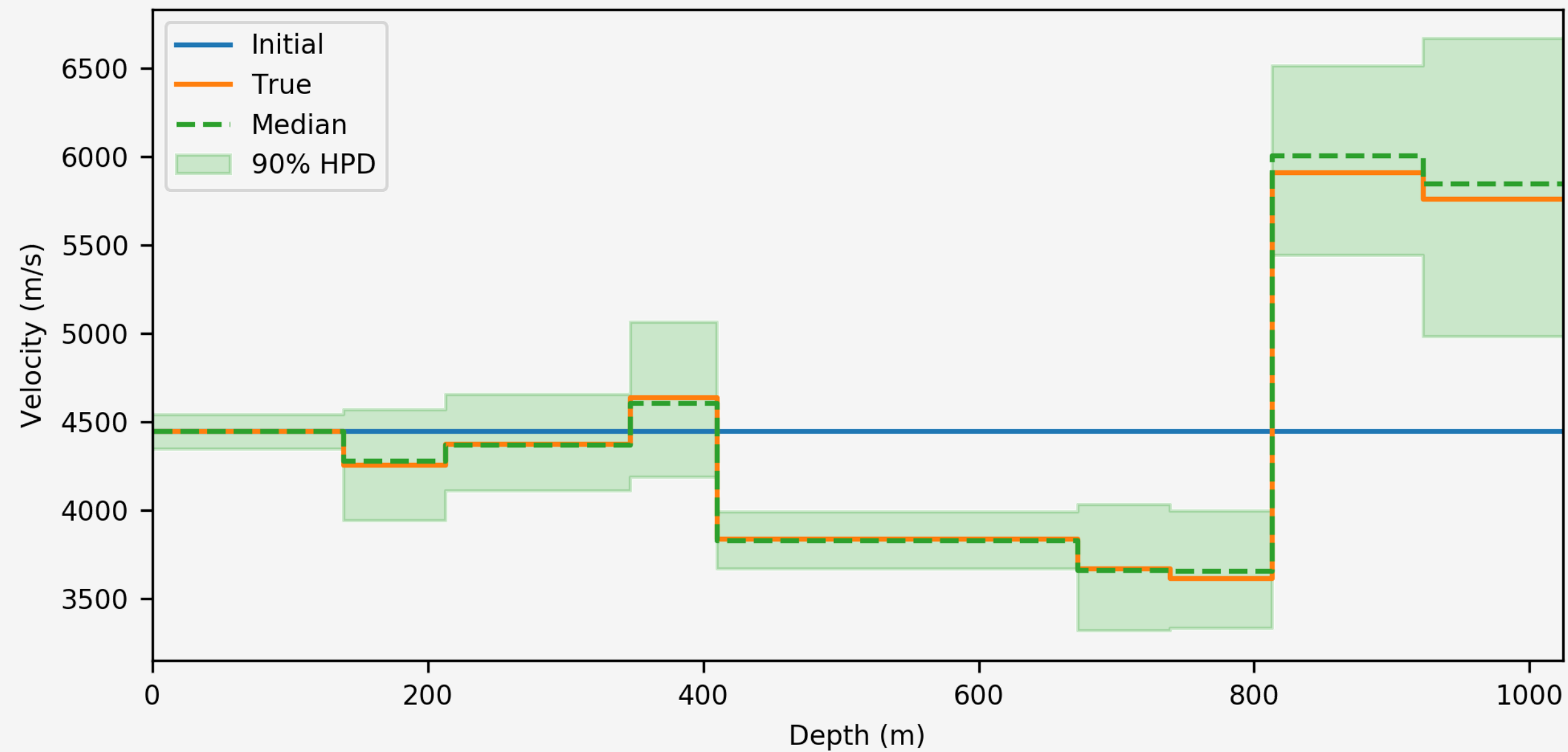


Figure: A vertical slice of the initial (blue), true (orange), and median (green dashed) velocity fields. With 90% highest posterior density intervals.

TROUBLE: THE RANDOM WALK SAMPLER



- ✓ In **theory**, MCMC will converge to the target distribution.
- ✓ In **practice**, methods based on random walk sampling (RWS) can handle a limited number of unknowns (**< 100 in our experience**)
- ✓ RWS produces samples that are highly **correlated**.¹

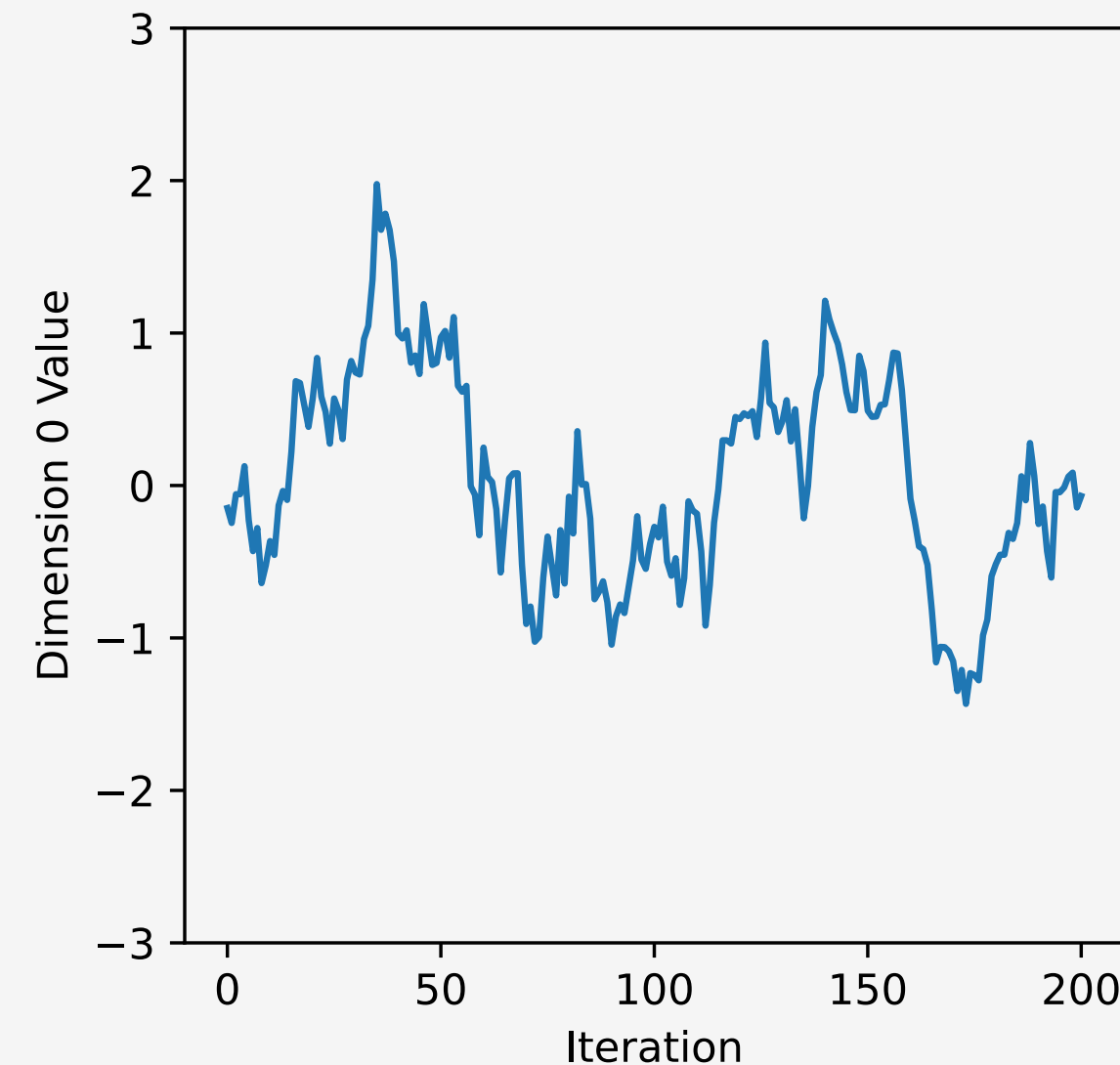


Figure: A view of one dimension of a 100-dimensional Gaussian sampled with Metropolis-Hastings MCMC.

THE RANDOM WALK SAMPLER
PRACTICALLY LIMITS THE
NUMBER OF UNKNOWNNS WE
CAN USE

- ✓ HMC uses **Hamiltonian Mechanics** and **gradient information** of the posterior distribution to draw samples that are less correlated.
- ✓ This results in an algorithm that can handle **higher dimensions** and **converges in fewer samples**.

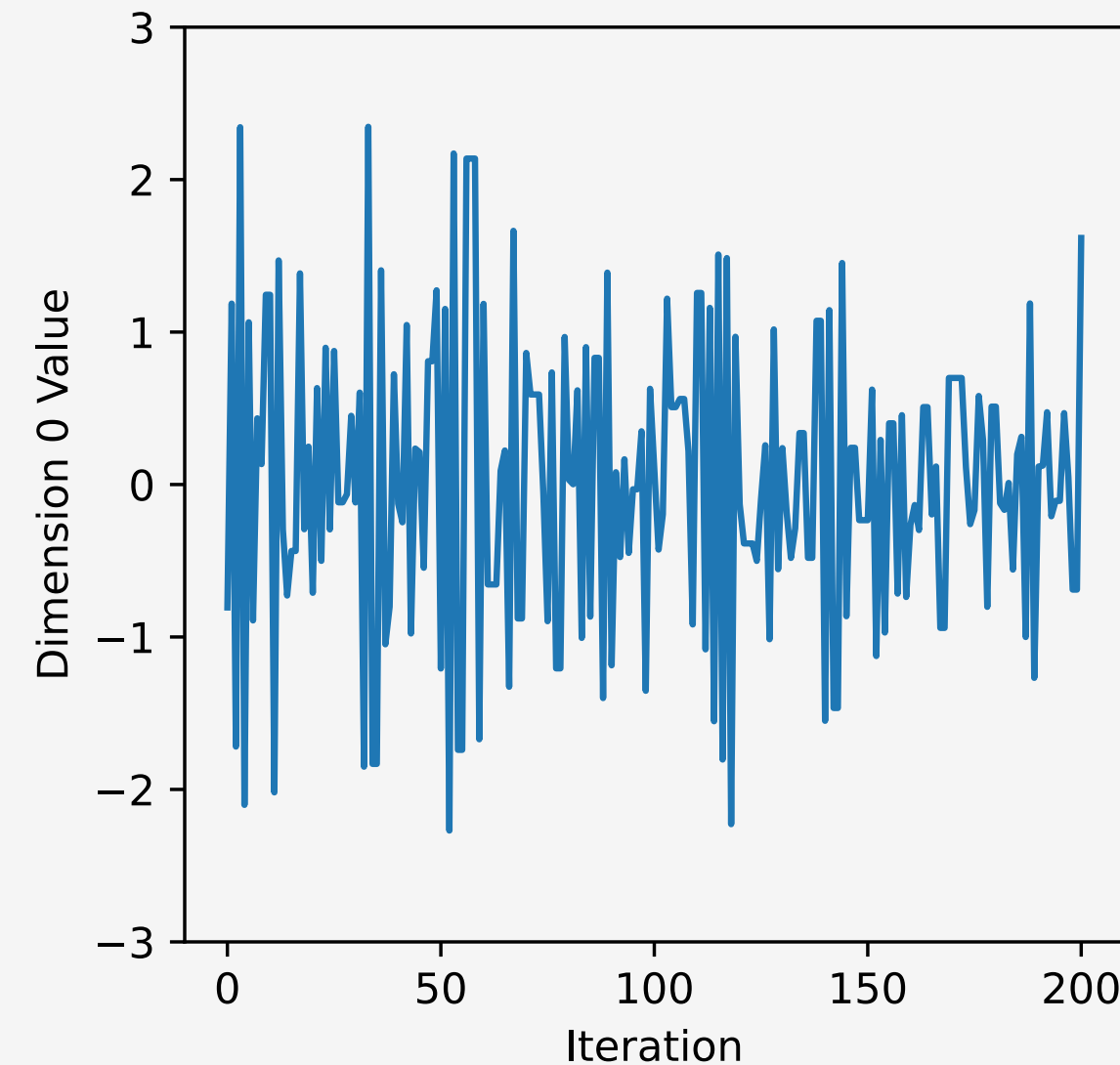


Figure: A view of one dimension of a 100-dimensional Gaussian sampled with HMC.

Potential
Energy

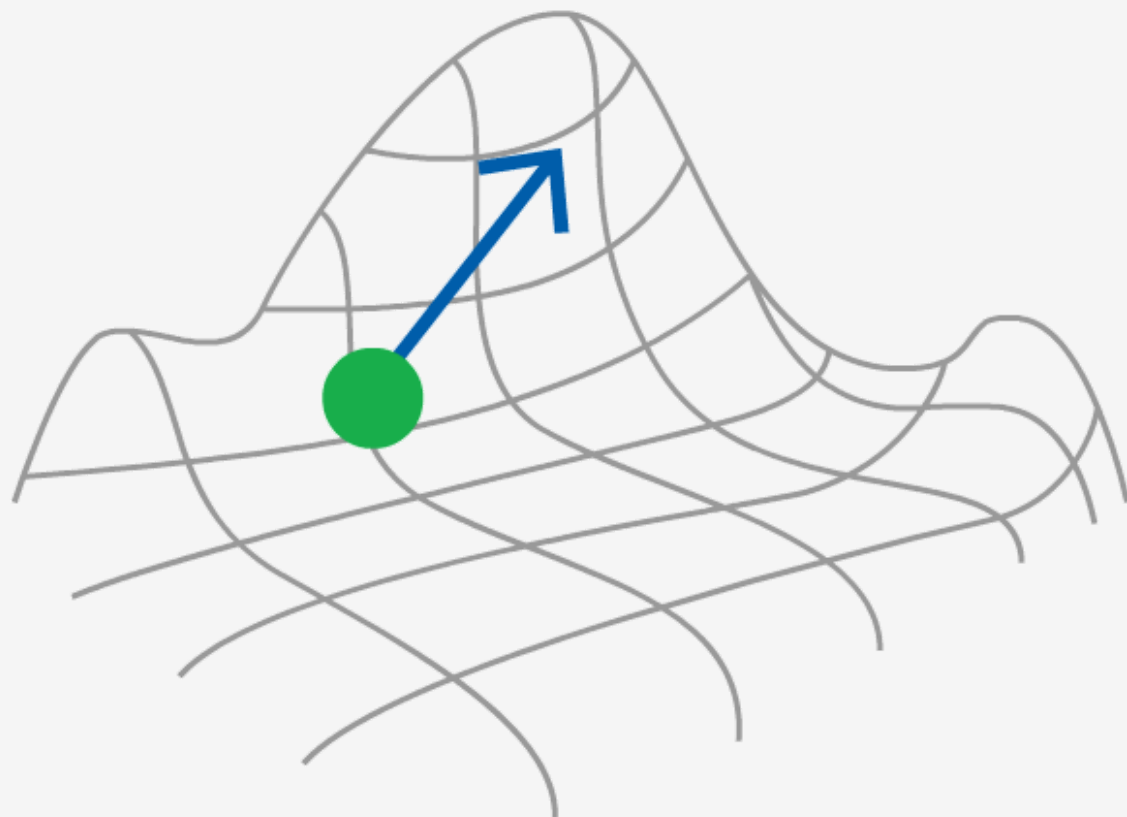
Kinetic Energy

$$H(q, p) = U(q) + K(p)$$

Hamiltonian

Position

Momentum



HAMILTON'S EQUATIONS AND THE POSTERIOR DISTRIBUTION



✚ The posterior distribution is embedded in the potential energy by way of the **canonical distribution**.

$$U(q) = -\log[\pi(q|D)] = -\log[\pi(q)\pi(D|q)]$$

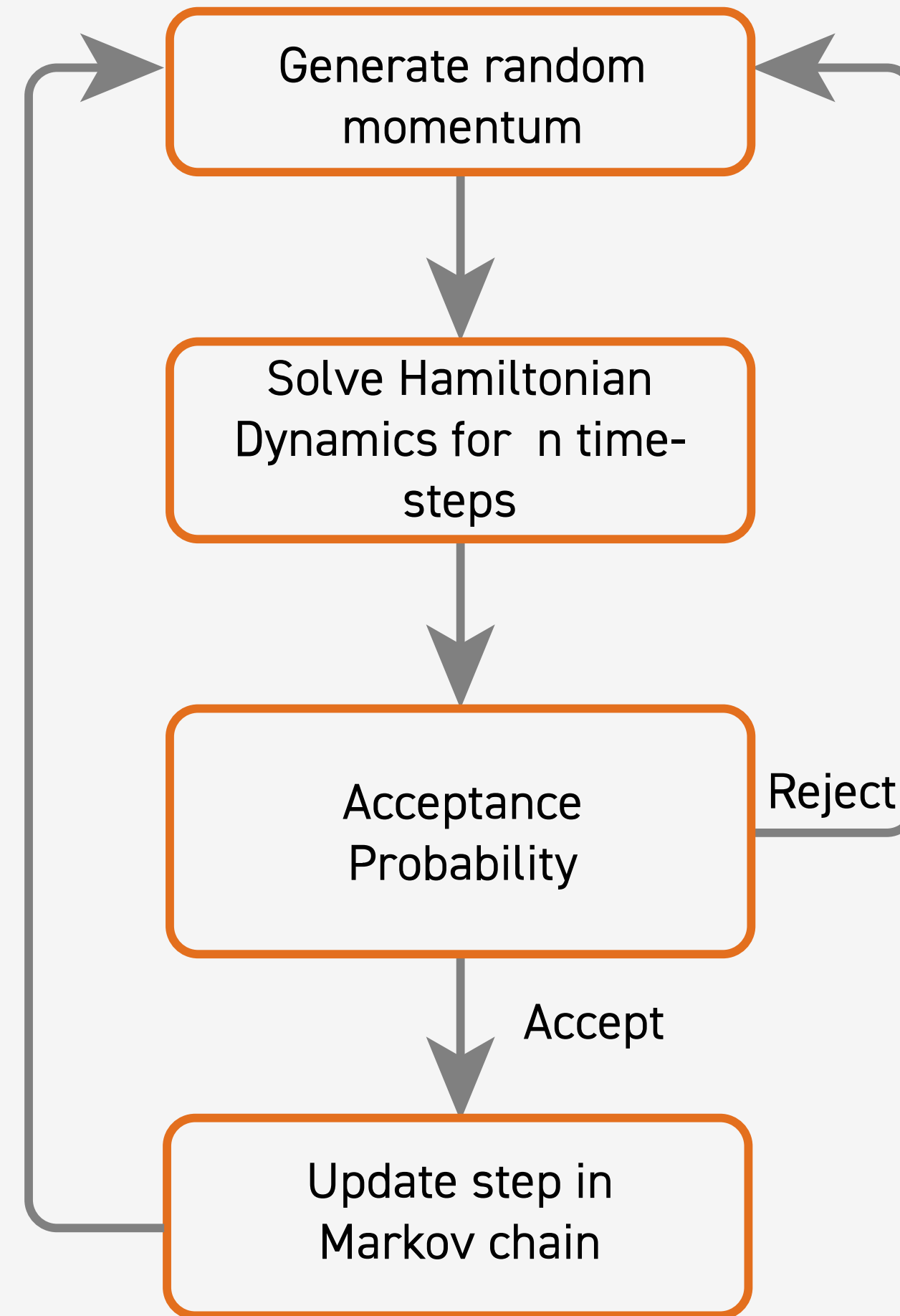
where $\pi(q|D)$ is the **posterior distribution**, $\pi(q)$ is the **prior distribution**, and $\pi(D|q)$ is the **likelihood function**.

✚ For Hamilton's equations, we need to take the **gradient of the log likelihood**.

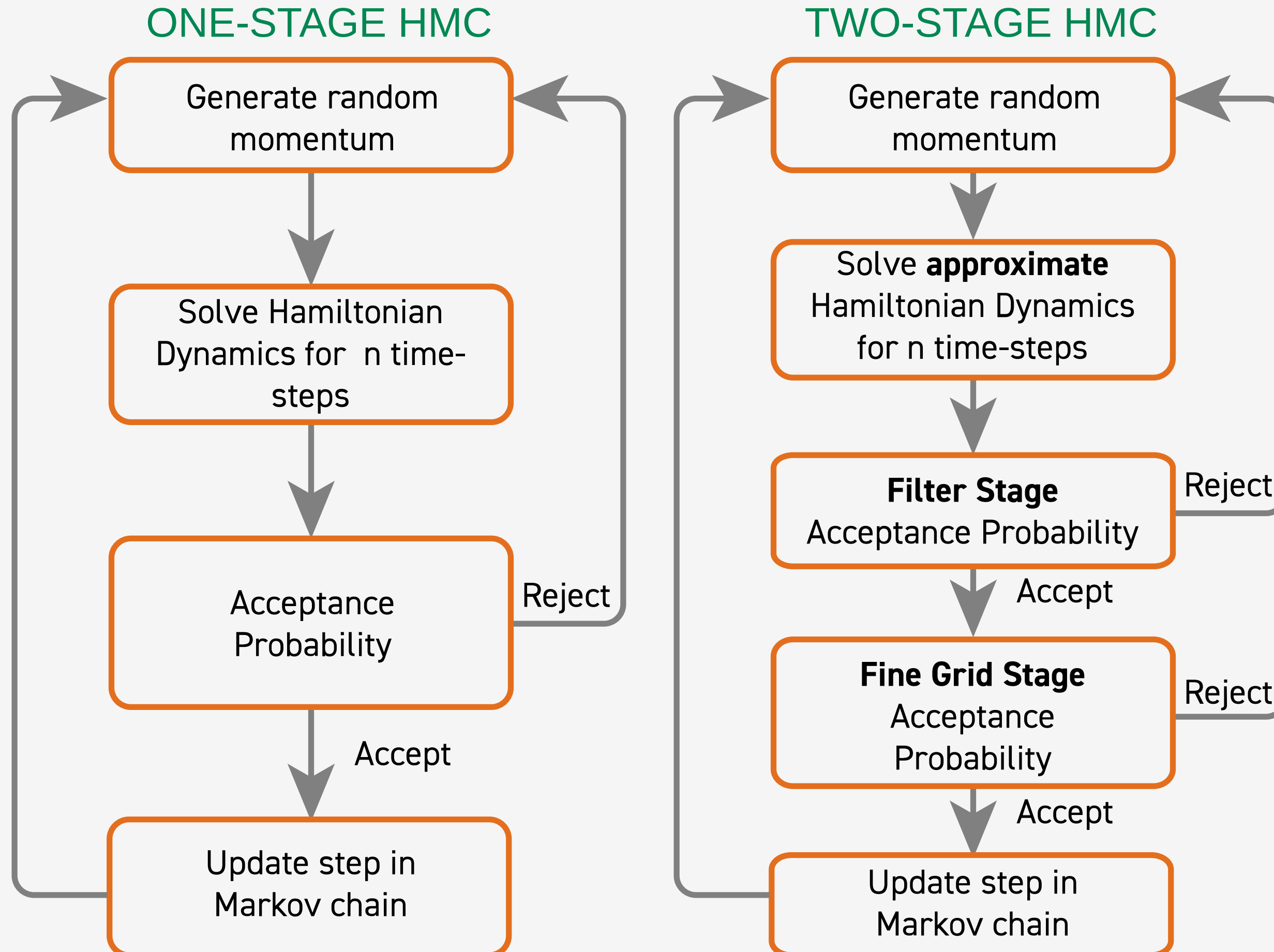
$$-\nabla \log[\pi(D|q)] = \nabla \frac{\|F(q) - D\|^2}{2\sigma^2}$$

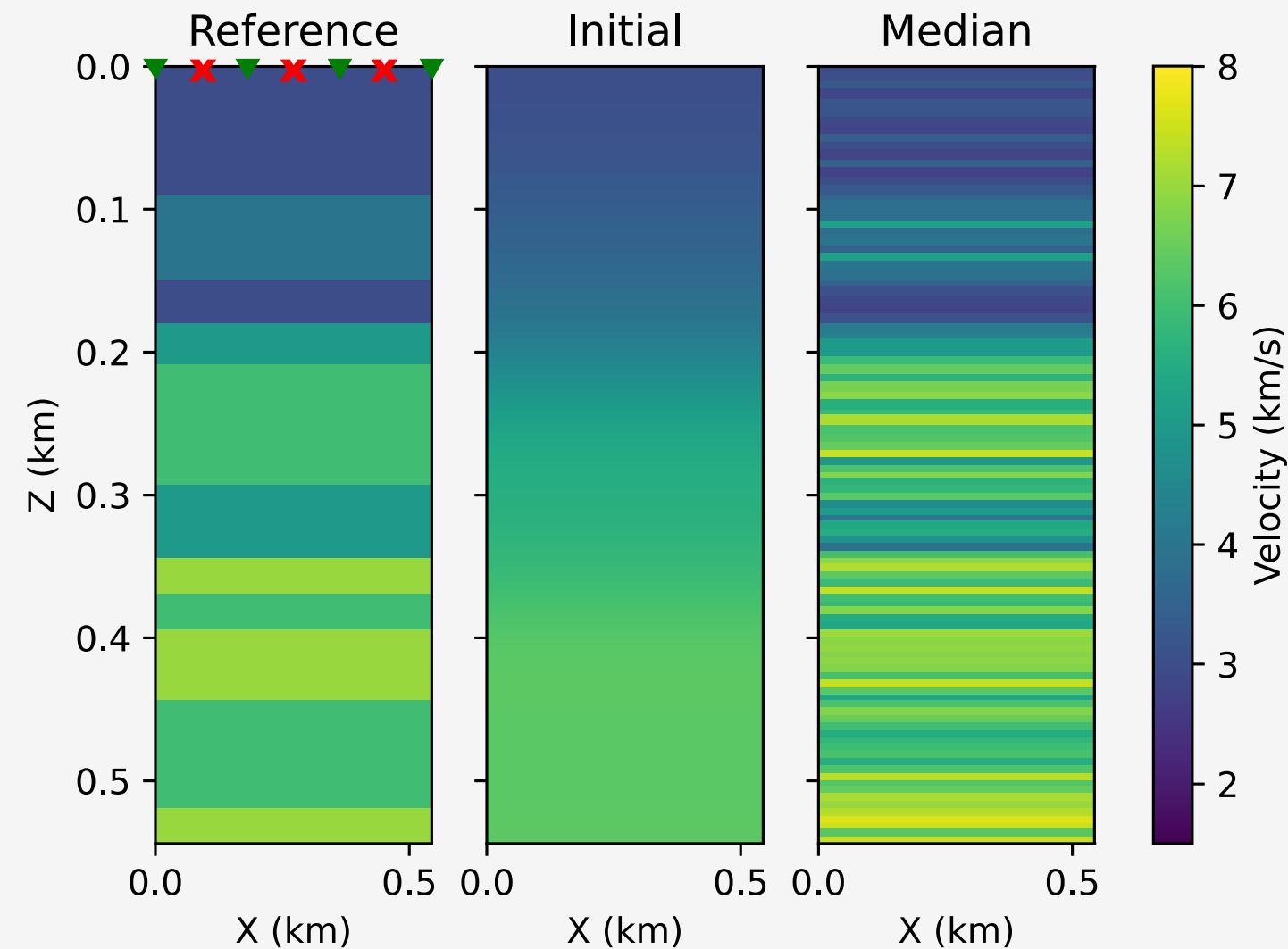
THE LEAPFROG DISCRETIZATION





HAMILTONIAN MONTE CARLO
REQUIRES NUMEROUS
EXPENSIVE GRADIENT
CALCULATIONS TO PRODUCE
EACH SAMPLE.





⚡ All timings include
generating the training
set and training the
neural network.

⚡ Time-per-trial
decreased by 85%.

Figure: The initial (left), true (middle), and median (right) velocity fields for the 100-unknown neural net two-stage HMC experiment. On the left image, red x's represent a line of sources and green triangles represent a line of receivers.

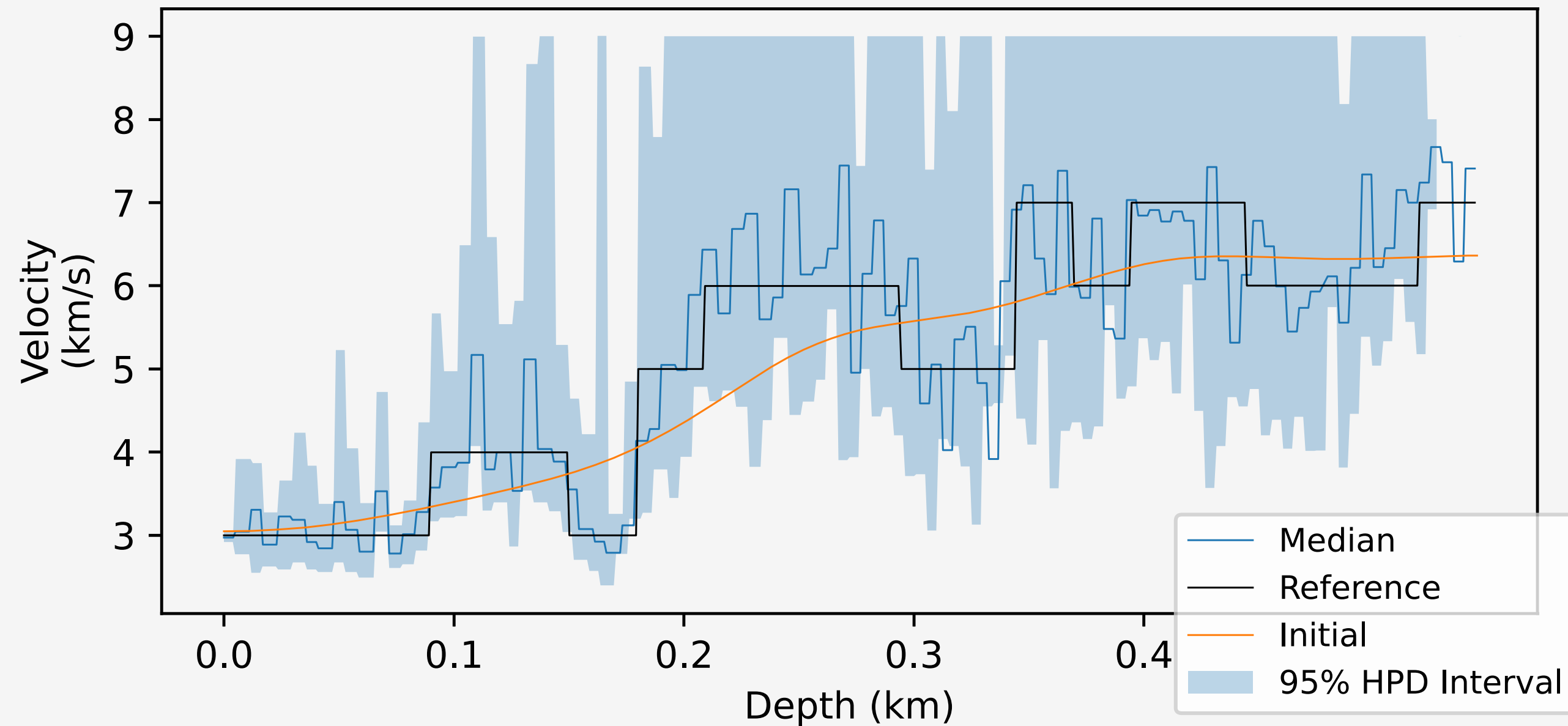


Figure: A one-dimensional slice of the median (blue), reference (black), and initial (orange) velocity fields, with 95% HPD interval shown with blue shading.

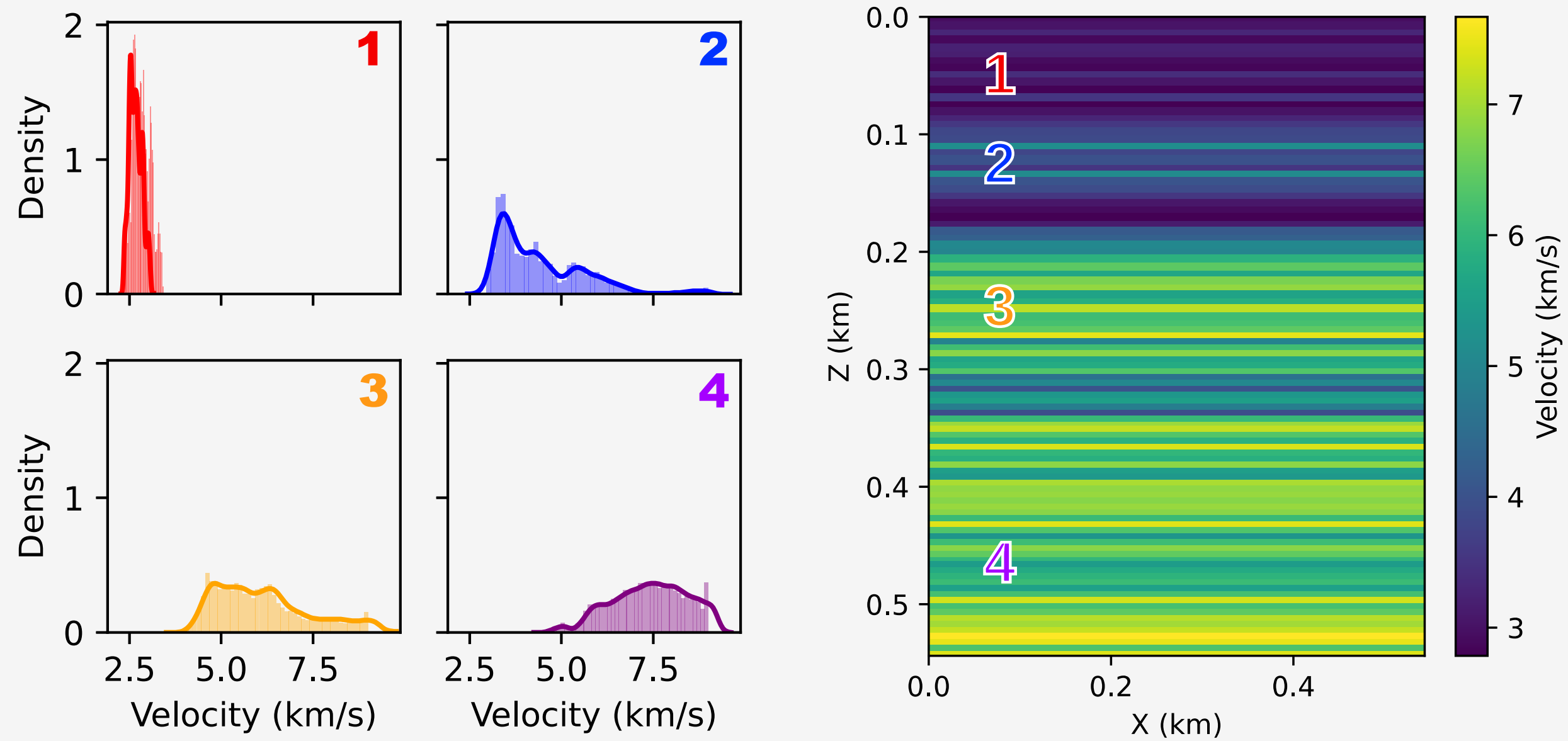


Figure: Four representative posterior distributions (left) from the marked locations (right).

HMC REQUIRES USER-
SPECIFIED PARAMETERS TO
DISCRETIZE THE HAMILTONIAN
DYNAMICS

- ✚ The **No-U-Turn Sampler (NUTS)** modifies HMC to have an adaptive trajectory length L .
- ✚ **Eliminates costly tuning runs** for the trajectory length in the leapfrog algorithm.
- ✚ From the starting point (blue dot), we **we randomly select a forward trajectory** (yellow dot) or a **backward trajectory** (green dots).
- ✚ The number of leapfrog steps **doubles** with each recursive NUTS iteration.



NUMERICAL EXPERIMENT: NUTS

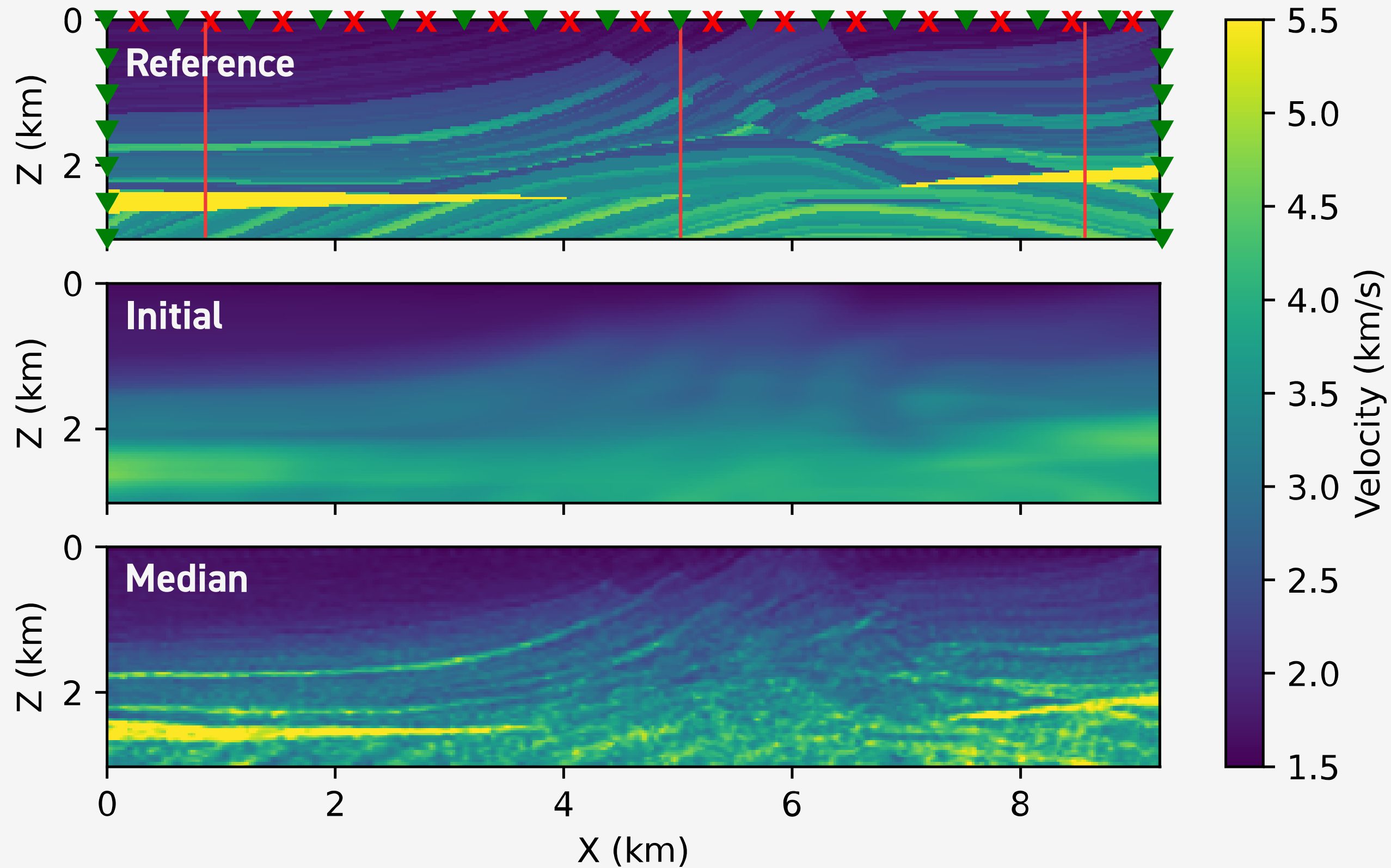
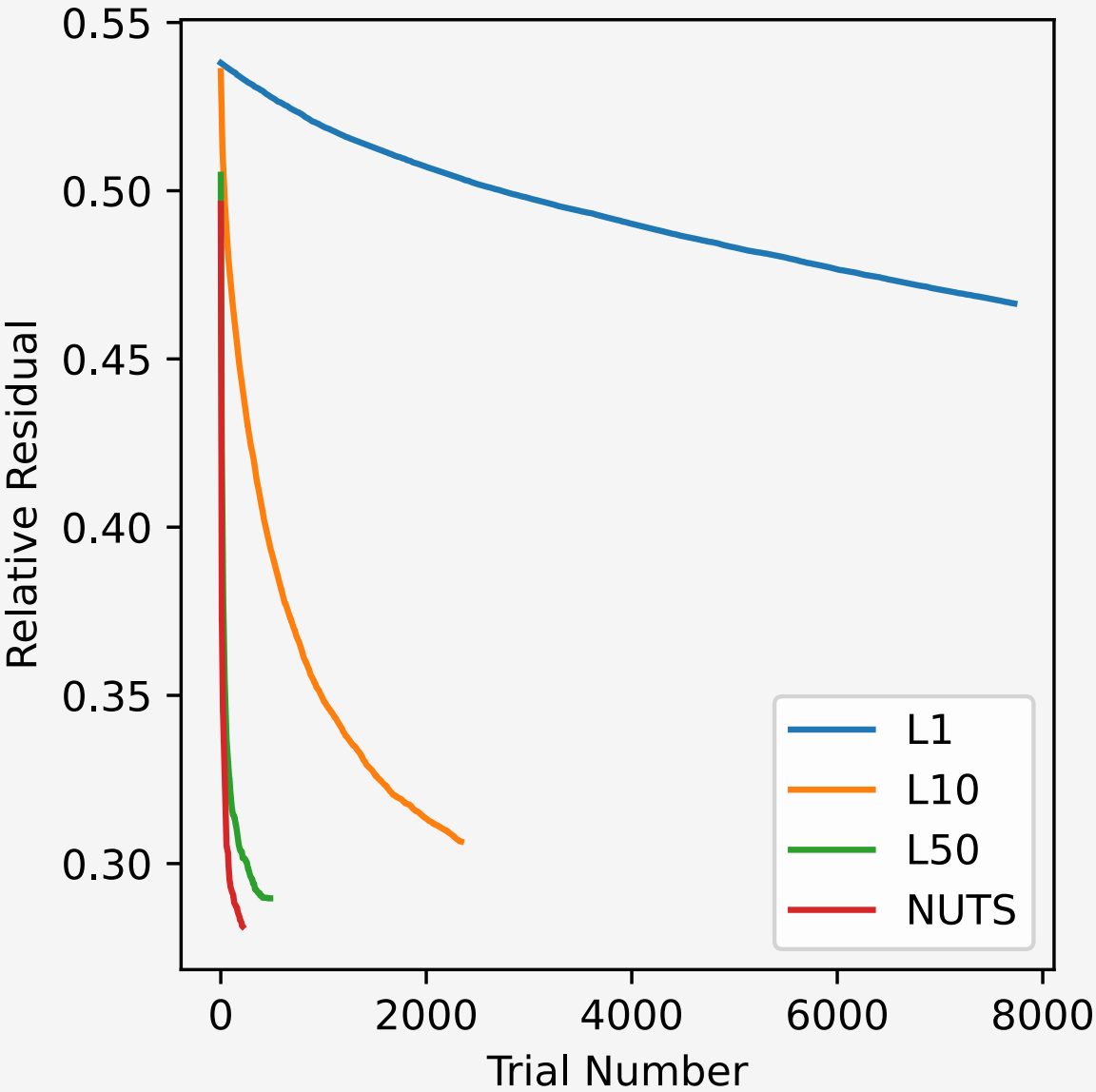


Figure: Top: the reference velocity field with markings for sources (red X's) and receivers (green triangles) and red lines to mark the location of the vertical slices (next slide). Middle: The initial velocity field. Bottom: the median velocity field.



⚡ We find that the NUTS algorithm results in superior residual decrease while maintaining a high acceptance rate.

⚡

Leapfrog Steps	Acceptance Rate
1	0.72
10	0.66
50	0.35
NUTS	0.98

Figure: Relative residual plots for leapfrog step number 1 (blue), 10 (orange), 50 (green), and the NUTS algorithm (red).

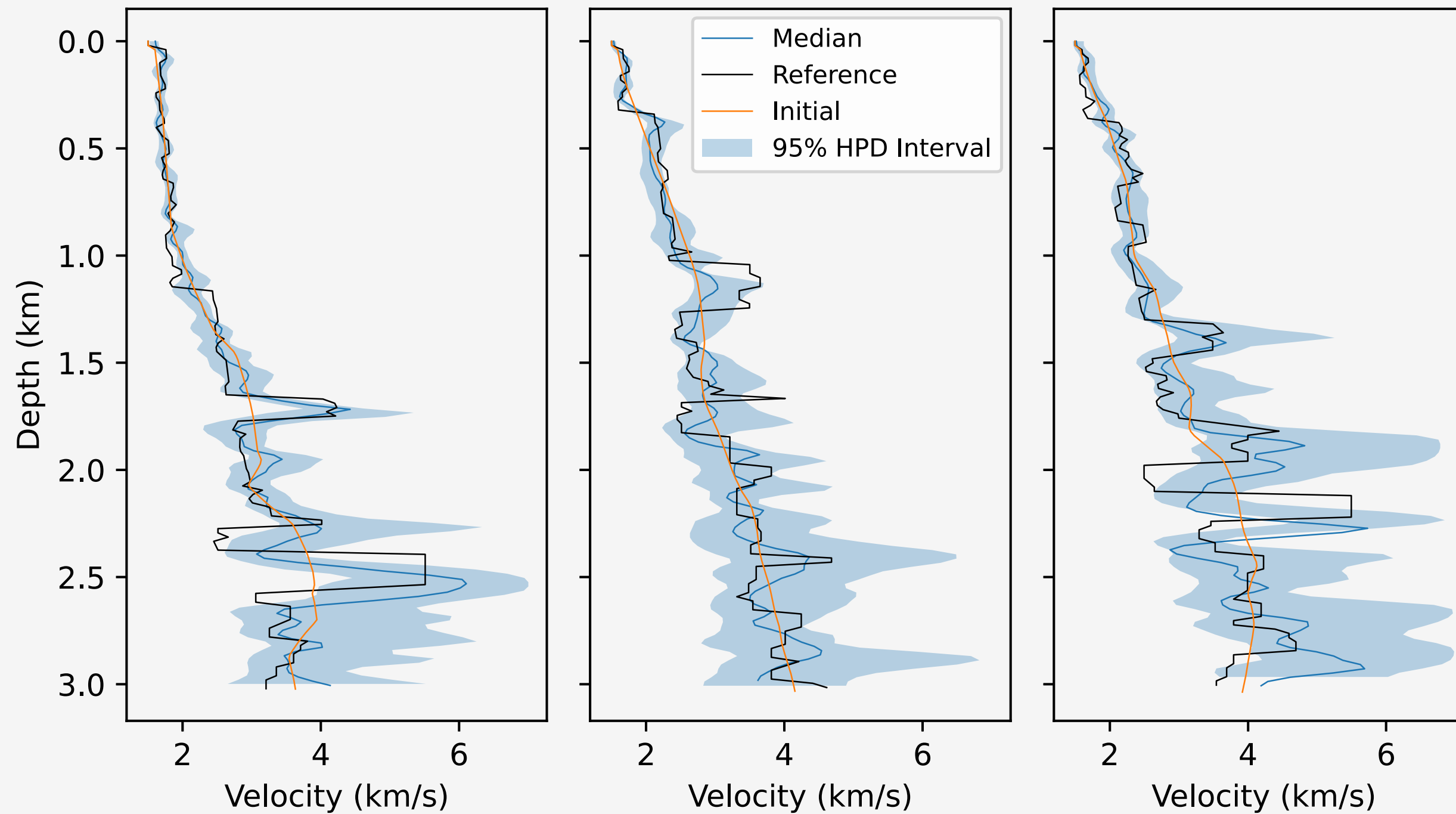


Figure: Vertical slices of the median (blue), reference (black), and initial (orange) velocity fields at locations shown on the previous slide. The blue shaded region marks the 95% HPD intervals

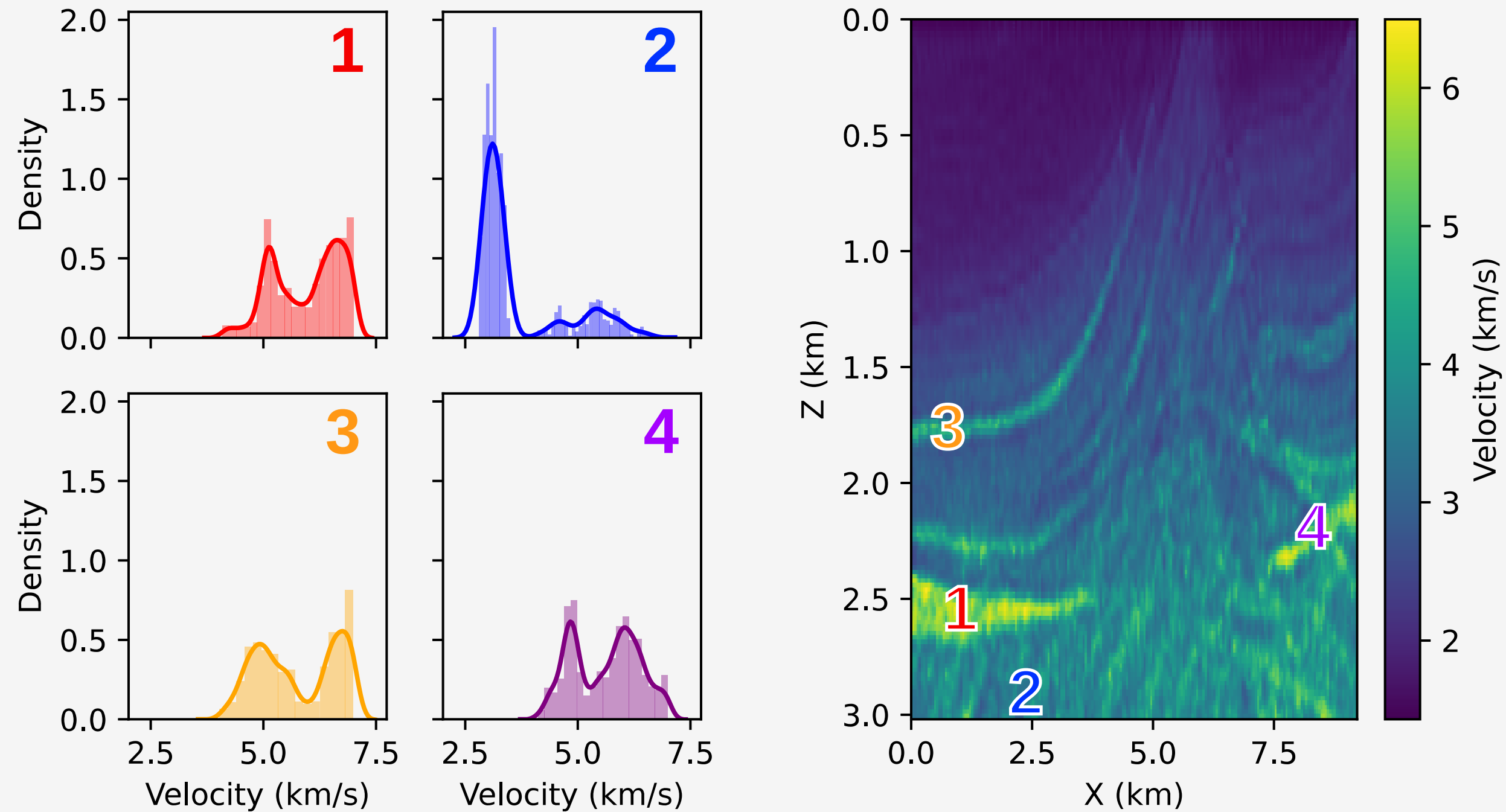


Figure: Four representative posterior distributions (left) at the marked locations shown on the right figure.

- ✚ Two-stage MCMC and HMC is an effective way to quickly reject unacceptable samples and to reduce runtime of the **expensive MCMC and HMC procedures**.
- ✚ **Operator upscaling** is a highly accurate surrogate that closely replicates the fine-grid receiver data.
- ✚ A **neural net** is an extremely inexpensive surrogate that can do a good job of approximating the exponent of the **likelihood function** and the **likelihood gradient**.
- ✚ **Neural-Net Enhanced HMC** reduces the run-time of the HMC algorithm by **over 80%** for our experiment.
- ✚ **The No-U-Turn sampler** optimizes the leapfrog trajectory length for HMC.








- √ We recently extended the two-stage HMC framework to the NUTS algorithm.
- √ Currently in progress: a paper on neural-network enhanced two-stage HMC and NUTS.
- √ NNHMC/NNNUTS on larger-scale problems with tens of thousands of unknowns.
- √ Applying our methods to real data.

ACKNOWLEDGEMENTS



THANK YOU TO...

- ✿ my advisers, Sue Minkoff and Felipe Pereira.
- ✿ David Lumley and Hejun Zhu for use of the seismology group's HPC cluster.
- ✿ Chris Simmons and the Ganymede cluster team for HPC support.
- ✿ the sponsors of the UT Dallas 3D+4D seismic consortium for financial support and industry feedback throughout my research.
- ✿ the Enriched Doctoral Training (EDT) Program, DMS grant #1514808.
- ✿ Pioneer Natural Resources, in particular Rob Meek and Matt McChesney (now at Guidon Energy) for providing well log data and industry feedback.
- ✿ Tim Ullrich for supporting me and always listening to me talk about my research.

- 
 Christen, J. A., and C. Fox, 2005, [Markov chain Monte Carlo Using an Approximation](#): Journal of Computational and Graphical Statistics: A Joint Publication of American Statistical Association, Institute of Mathematical Statistics, Interface Foundation of North America, 14, 795–810.
- 
 Efendiev, Y., T. Hou, and W. Luo, 2006, [Preconditioning Markov Chain Monte Carlo Simulations Using Coarse-Scale Models](#): SIAM Journal on Scientific Computing: A Publication of the Society for Industrial and Applied Mathematics, 28, 776–803.
- 
 Hoffman, M. D., and A. Gelman, 2014, [The No-U-Turn sampler: adaptively setting path lengths in Hamiltonian Monte Carlo](#) : Journal of Machine Learning Research: JMLR, 15, 1593–1623.
- 
 Korostyshevskaya, O., and S. E. Minkoff, 2006, [A Matrix Analysis of Operator-Based Upscaling for the Wave Equation](#): SIAM Journal on Numerical Analysis, 44, 586–612.
- 
 Neal, R. M., 2011, [MCMC using Hamiltonian dynamics](#), in S. Brooks, A. Gelman, G. L. Jones, and X.-L. Meng, eds., Handbook of Markov Chain Monte Carlo. Handbooks of Modern Statistical MethodsChapman & Hall / CRC, 113–162.
- 
 Stuart, G. K., W. Yang, S. Minkoff, and F. Pereira, 2016, [A two-stage Markov chain Monte Carlo method for velocity estimation and uncertainty quantification](#), in SEG Technical Program Expanded Abstracts 2016, 3682–3687.
- 
 Stuart, G. K., S. E. Minkoff, and F. Pereira, 2019a, [Enhanced neural network sampling for two-stage Markov chain Monte Carlo seismic inversion](#): SEG Technical Program Expanded Abstracts 2019, 5, 1665–1669.
- 
 Stuart, G. K., S. E. Minkoff, and F. Pereira, 2019b, [A two-stage Markov chain Monte Carlo method for seismic inversion and uncertainty quantification](#): Geophysics, 84, R1015–R1032.
- 
 Vdovina, T., S. E. Minkoff, and O. Korostyshevskaya, 2005, [Operator Upscaling for the Acoustic Wave Equation: Multiscale Modeling & Simulation](#): A SIAM Interdisciplinary Journal, 4, 1305–1338.
- 
 Vdovina, T., and S. Minkoff, 2008, [An a priori error analysis of operator upscaling for the acoustic wave equation](#): International Journal of Numerical Analysis and Modeling, 5, 543–569.